



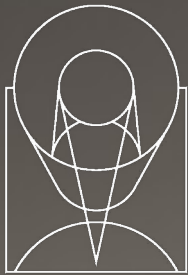
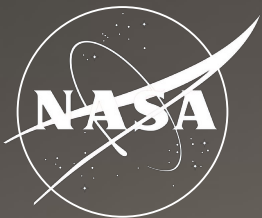
Stockholm
University



PRINCETON
UNIVERSITY

Direct & Indirect Detection of Dark Matter with Novel Targets: Why It Pays to Know a Chemist

CARLOS BLANCO



SPACE
TELESCOPE
SCIENCE
INSTITUTE

Our dark matter halo

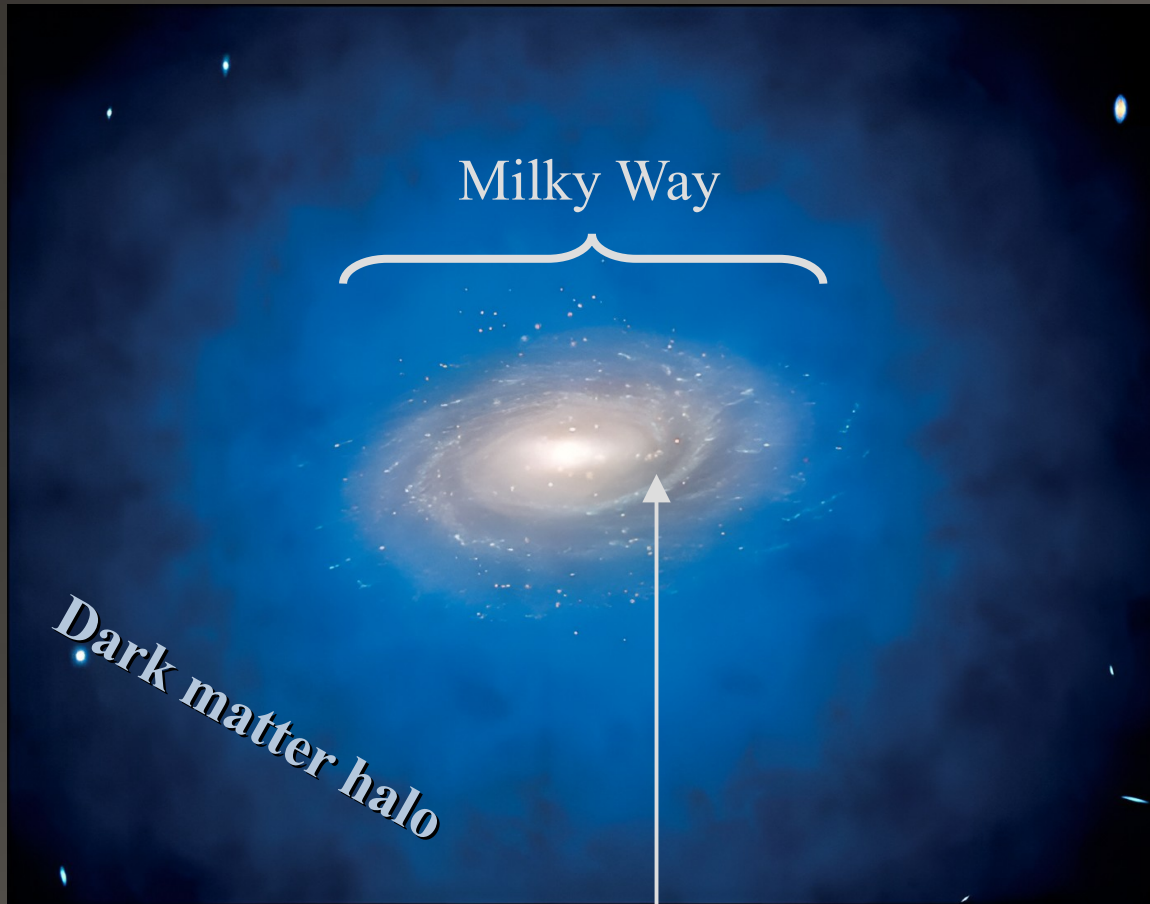


Image credit: ESO/L Calçada

We are here.

Observations of our galaxy tell us:

Local dark matter density

$$\rho_{\text{DM}} = 0.4 \text{ GeV}/\text{cm}^3$$

Local dark matter velocity

$$\langle v_{\text{DM}} \rangle \approx 300 \text{ km/s}$$

Lighter masses \rightarrow more particles

$$n_{\text{DM}} = \rho_{\text{DM}}/m_{\text{DM}}$$

More particles \rightarrow larger fluxes

$$\phi_{\text{DM}} \sim v_{\text{DM}} n_{\text{DM}}$$

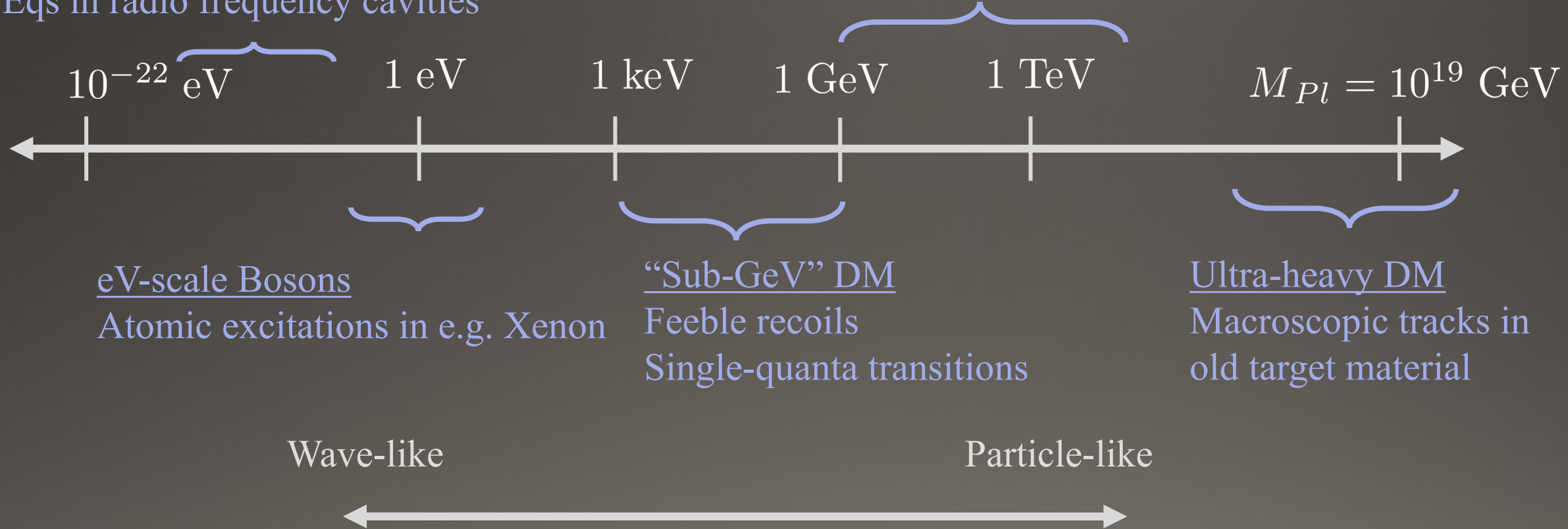
Detection pathways

Axions

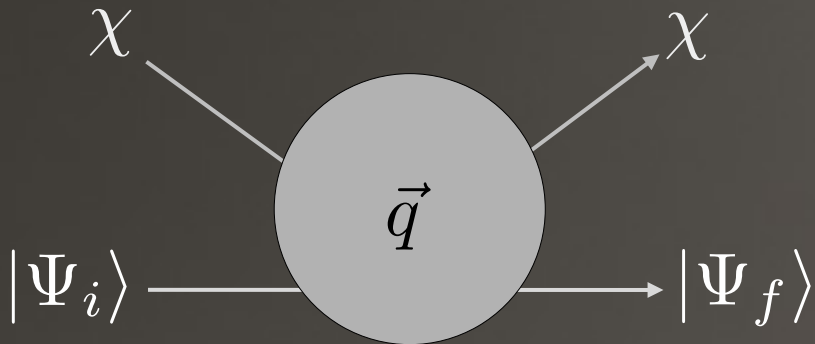
Effective changes to Maxwell's
Eqs in radio frequency cavities

Canonical WIMPs

Rare but energetic tracks in
cryogenic detectors.



Direct detection



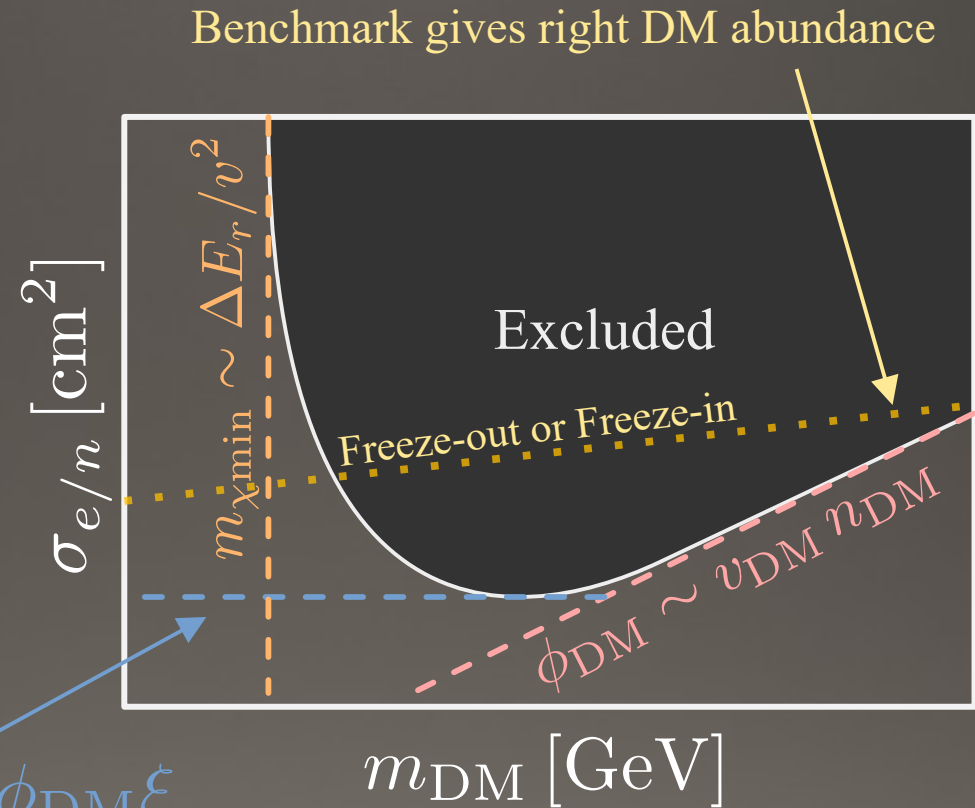
$$\bar{R}_{\text{sig}} \sim \xi \phi_{\text{DM}} \sigma \gtrsim \bar{R}_{\text{bkg}}$$

ξ : Signal generation efficiency

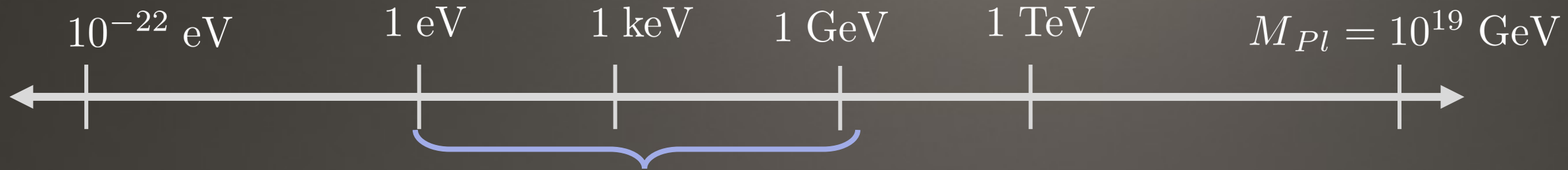
What we need is:

- Small threshold energies
- Large signal efficiencies
- Low backgrounds

$$\sigma_{\text{min}} \gtrsim \bar{R}_{\text{bkg}} / \phi_{\text{DM}} \xi$$



Sub-GeV direct detection



eV-scale Bosons & “Sub-GeV” DM

Classically allowed absorption & Inelastic scattering in *molecules* and *nanomaterials*

Kinetic energy of the dark matter

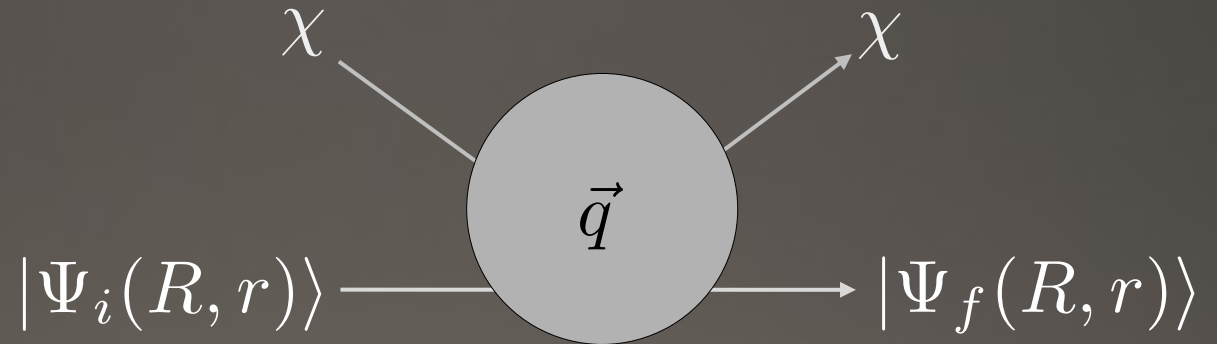
$$\Delta E \sim 10^{-6} m_\chi \approx \mathcal{O}(\text{eV}) \left(\frac{m_\chi}{1 \text{ MeV}} \right)$$

Imparted momentum in scattering

$$|q| \sim m_\chi v_\chi \approx \mathcal{O}(\text{keV}) \left(\frac{m_\chi}{1 \text{ MeV}} \right)$$

Imparted energy and momentum in absorption

$$|q| \approx 0, \quad \Delta E = m_\chi (\mathcal{O}(\text{eV}))$$



R : Nuclear coordinates

r : Electron coordinates

Interaction Rate

Rate “spectrum” (events in detector)

$$\frac{dR}{d \ln E_r} \sim \int \frac{d^3 \vec{q}}{q} \eta(v) |F_{\text{DM}}(q)|^2 |f_{i \rightarrow f}(q)|^2$$

Mean inverse velocity (Astro)

$$\eta(v)$$

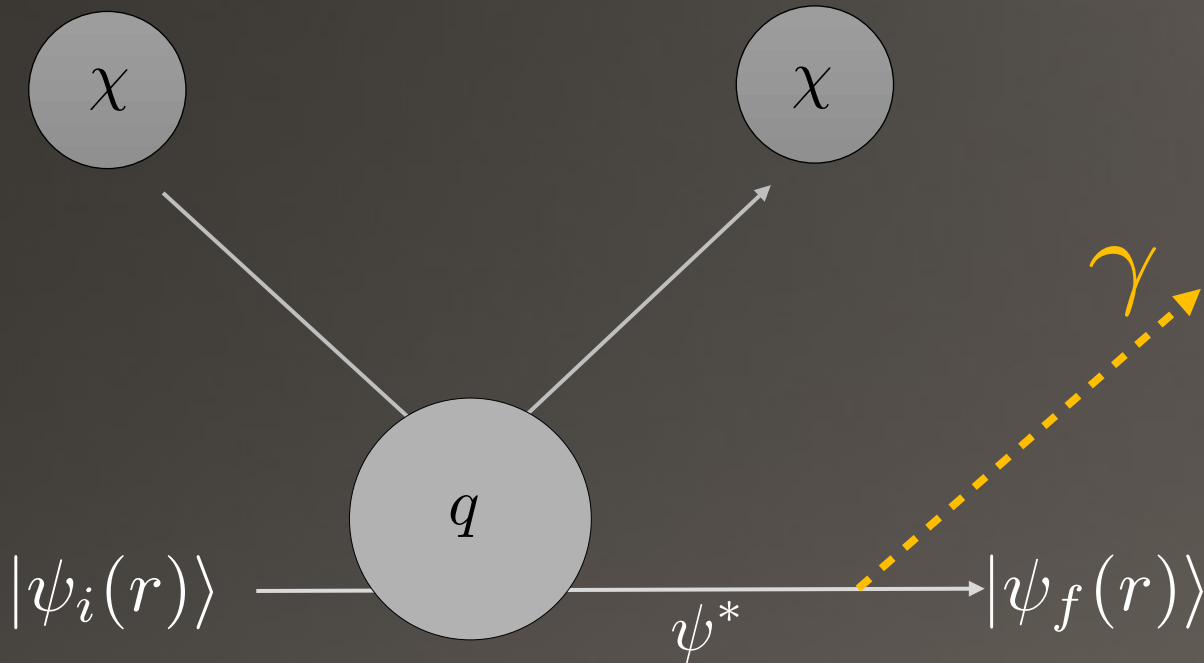
Transition form factor (Condensed matter / Chemistry)

$$f_{i \rightarrow f}(q) = \langle \Psi_f | e^{i\vec{q} \cdot \vec{r}} | \Psi_i \rangle = \langle \tilde{\Psi}_f(k + q) | \tilde{\Psi}_i(k) \rangle$$

Dark matter form factor (Particle physics)

$$F_{\text{DM}}(q) = \begin{cases} 1 & , \text{Contact interaction} \\ \left(\frac{\alpha m_e}{q} \right)^2 & , \text{Long-range interaction} \end{cases}$$

Electron Recoil: Photon Signal



Electron scattering or bosonic absorption leads to an excitation that decays via radiative emission.

A small unit that de-excites by emitting a photon is called a *chromophore*.

Electrons in crystals (exciton generation)

$$|\psi_i\rangle \sim u_v(r)e^{ik \cdot r} \quad |\psi\rangle^* \sim u_c(r)e^{ik \cdot r}$$

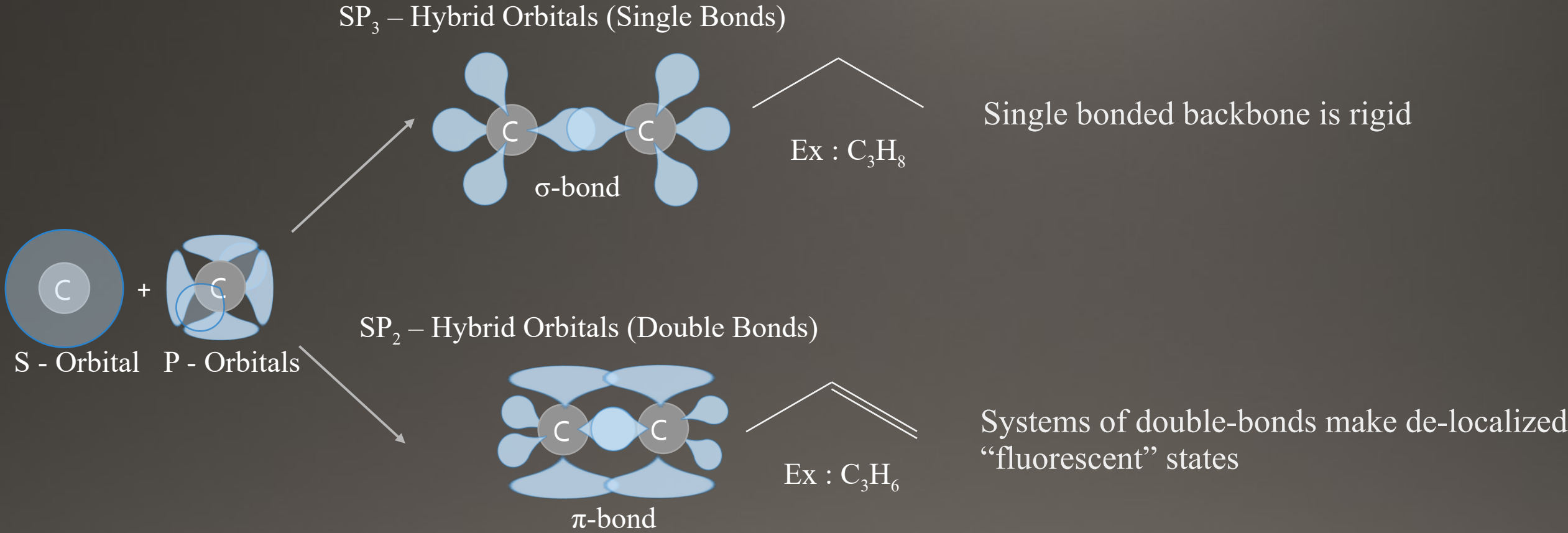
Excite from valence to conduction

Electrons in molecules and atoms

$$|\psi_i\rangle \sim \psi_{lcao}(r) \quad |\psi\rangle^* \sim \psi_{lcao}^*(r)$$

Excite quantized levels

Carbon: a natural candidate

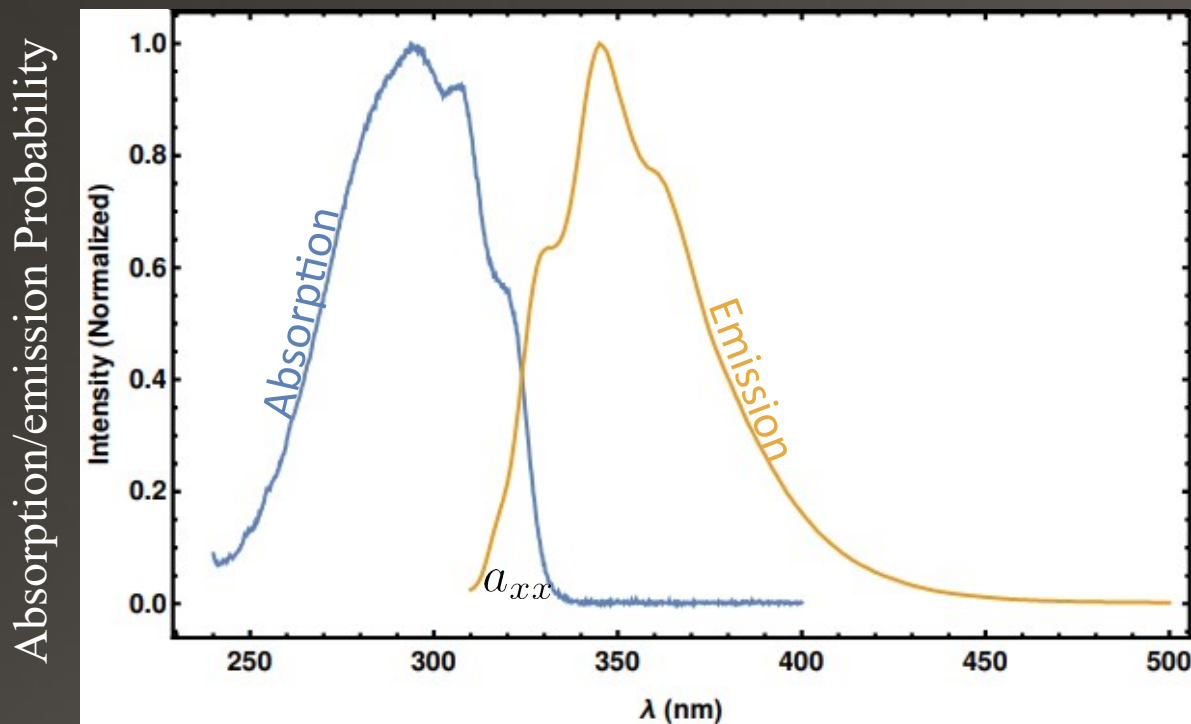


The de-localized p-orbital networks of carbon-based molecules are natural DM detector candidates

$$q_e \approx 1/a_0 \sim \mathcal{O}(\text{keV}) \qquad |q| \sim m_\chi v_\chi \approx \mathcal{O}(\text{keV}) \left(\frac{m_\chi}{1 \text{ MeV}} \right)$$

Fluorescence with DM

Characteristic fluorescence spectra of chromophores

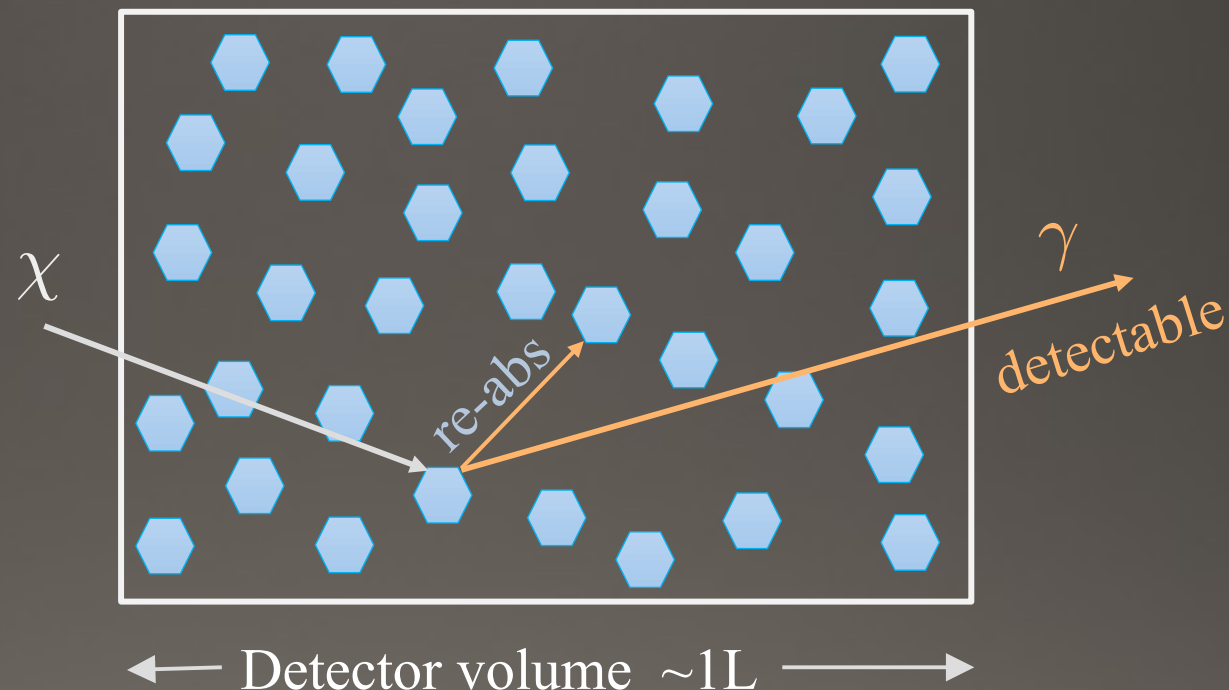


Decreasing energy (E) →

What we need is:

Large detectable signal efficiencies

Chromophore: 



Probability for the photon to free-stream

$$\Phi_{FB} \sim (1 - a_{xx})$$

Solid molecular crystals: $\Phi_{FB} \approx 65\%$

A pilot experiment

Problem: describe the interaction between DM (BSM) with molecules (chemistry)

Build the many body wave functions from molecular orbitals

$$\Psi_G = |\psi_2 \overline{\psi_2} \psi_1 \overline{\psi_1} \psi_1' \overline{\psi_1'}|$$

$$\Psi_i^j = \frac{1}{\sqrt{2}} (|\psi_1 \overline{\psi_1} \dots \psi_i \overline{\psi_j} \dots \psi_N \overline{\psi_N}| - |\psi_1 \overline{\psi_1} \dots \psi_j \overline{\psi_i} \dots \psi_N \overline{\psi_N}|)$$

Compute the molecular form factors

$$f_i(\mathbf{q}) = \int d^3 \mathbf{p} \tilde{\psi}_n(\mathbf{p}) \tilde{\psi}_{n+i}^*(\mathbf{p} + \mathbf{q})$$

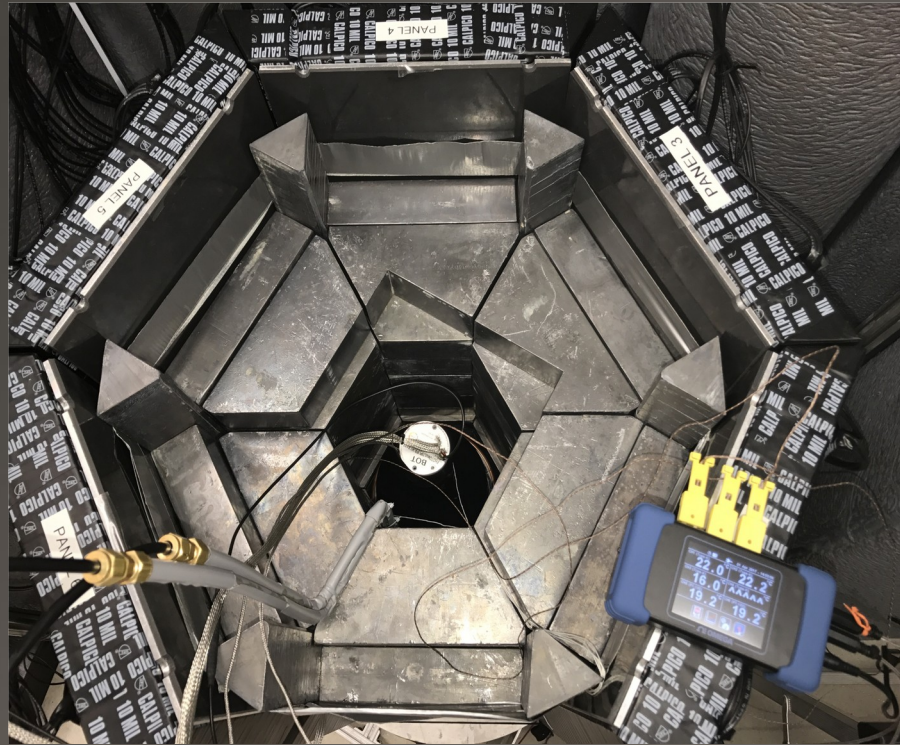
Para-xylene (EJ-301)



Commercially available

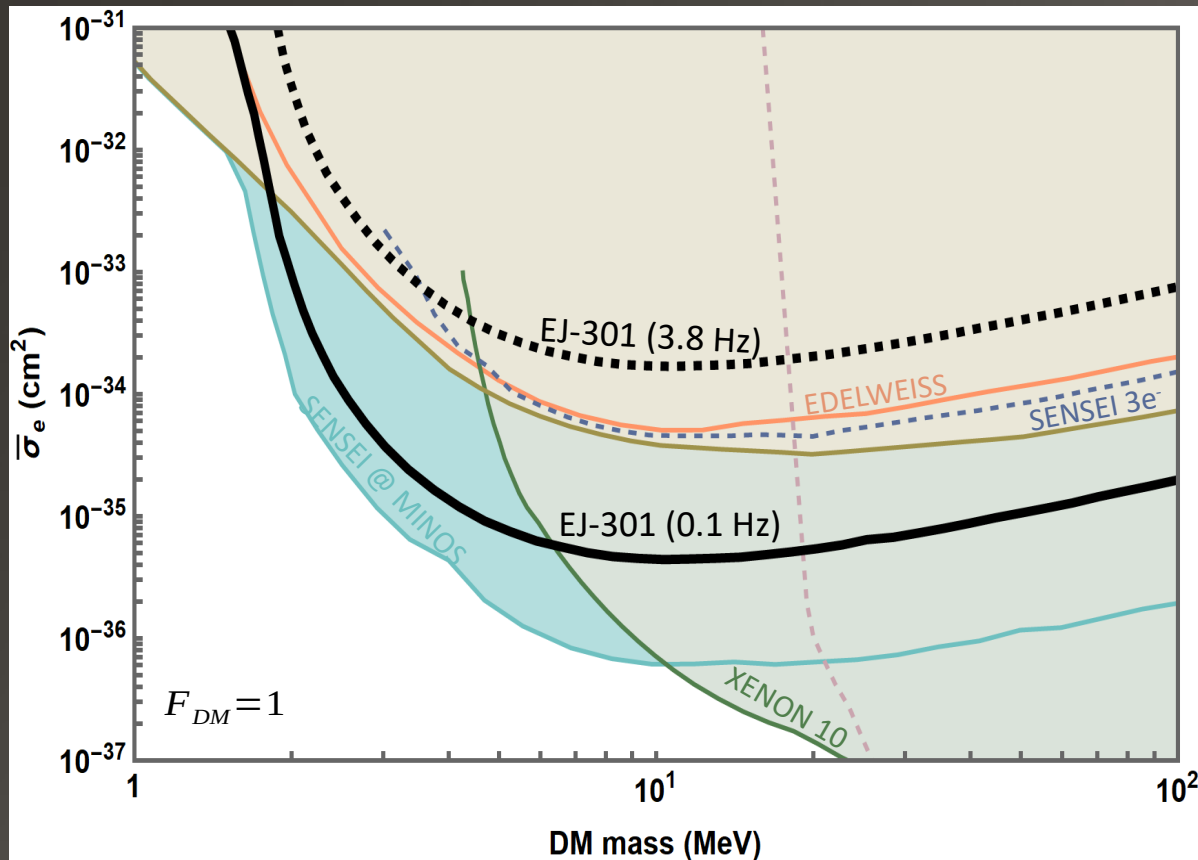
Molecular scintillators are cheap, well characterized, and extremely clean.

First Experimental Setup

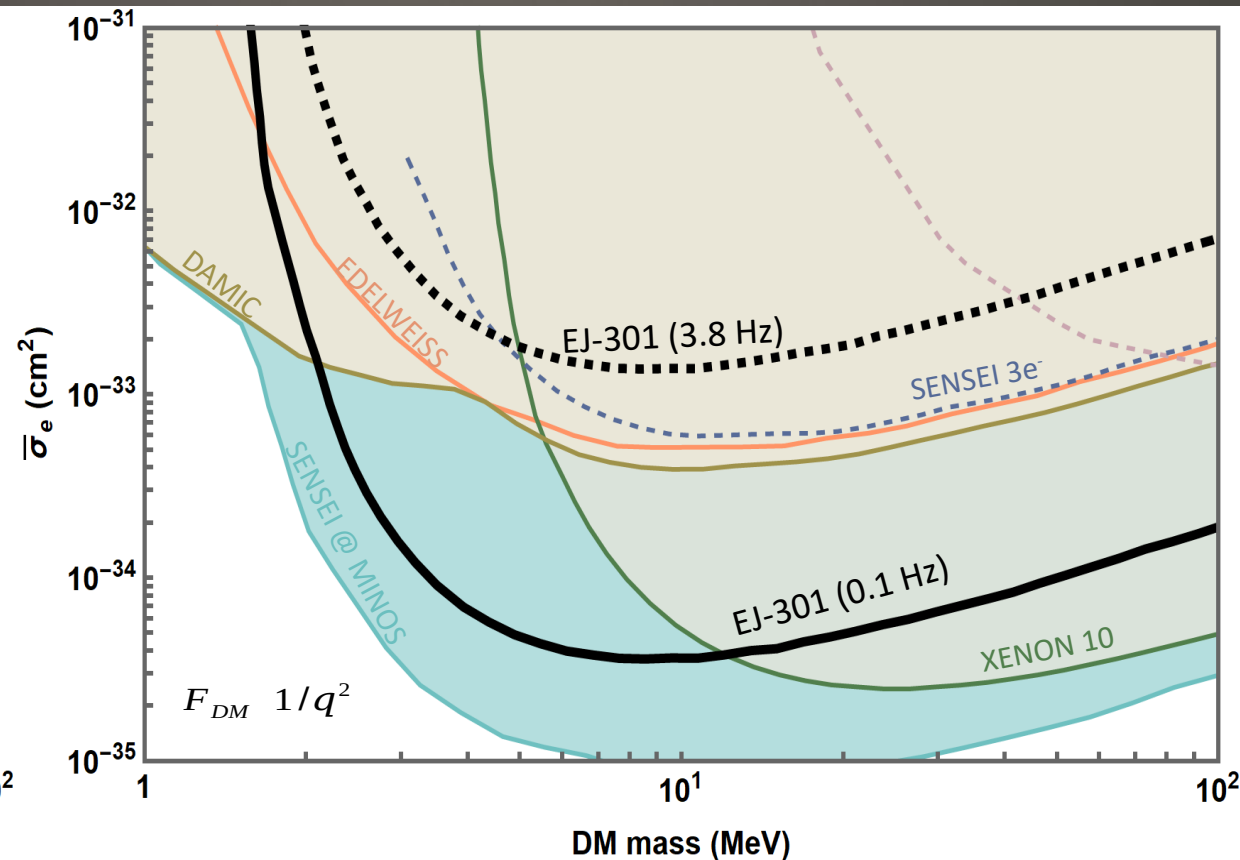


Results: EJ-301

(Contact interaction)



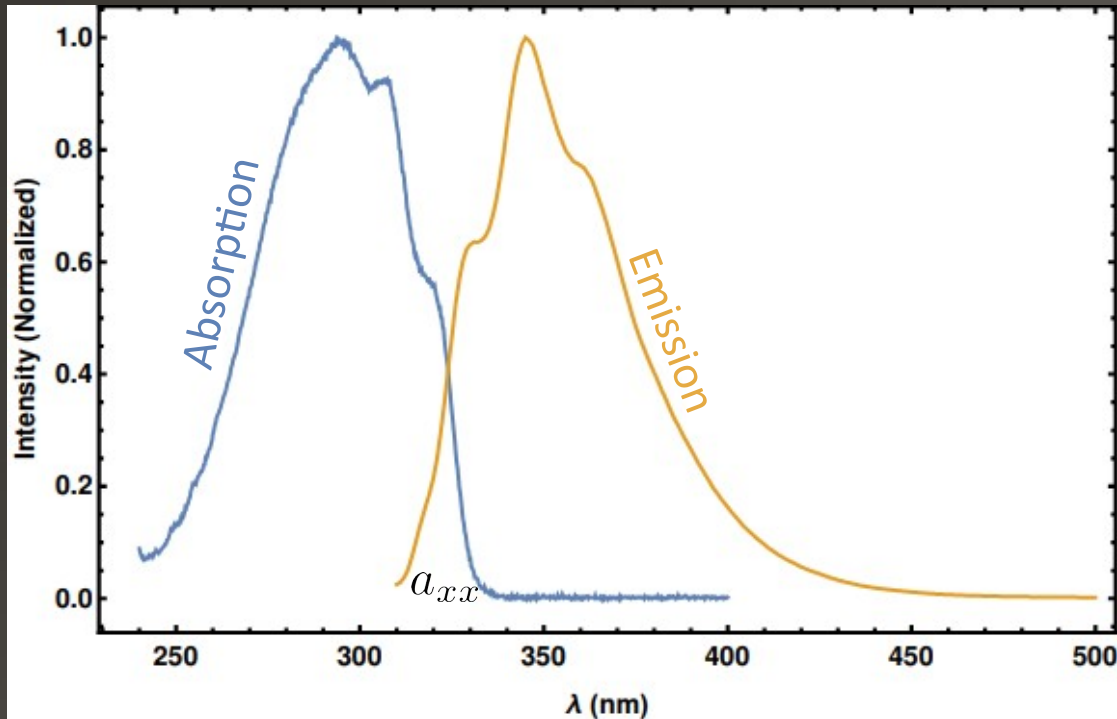
(Long-range interaction)



[CB, Collar, Kahn, Lillard: 1912.02822]

About 6 months from theory development to results!

Fluorescence with DM Works



Now what we need is:

Lower background

Option 1

Reduce background in the absorption step, i.e. selective excitation.

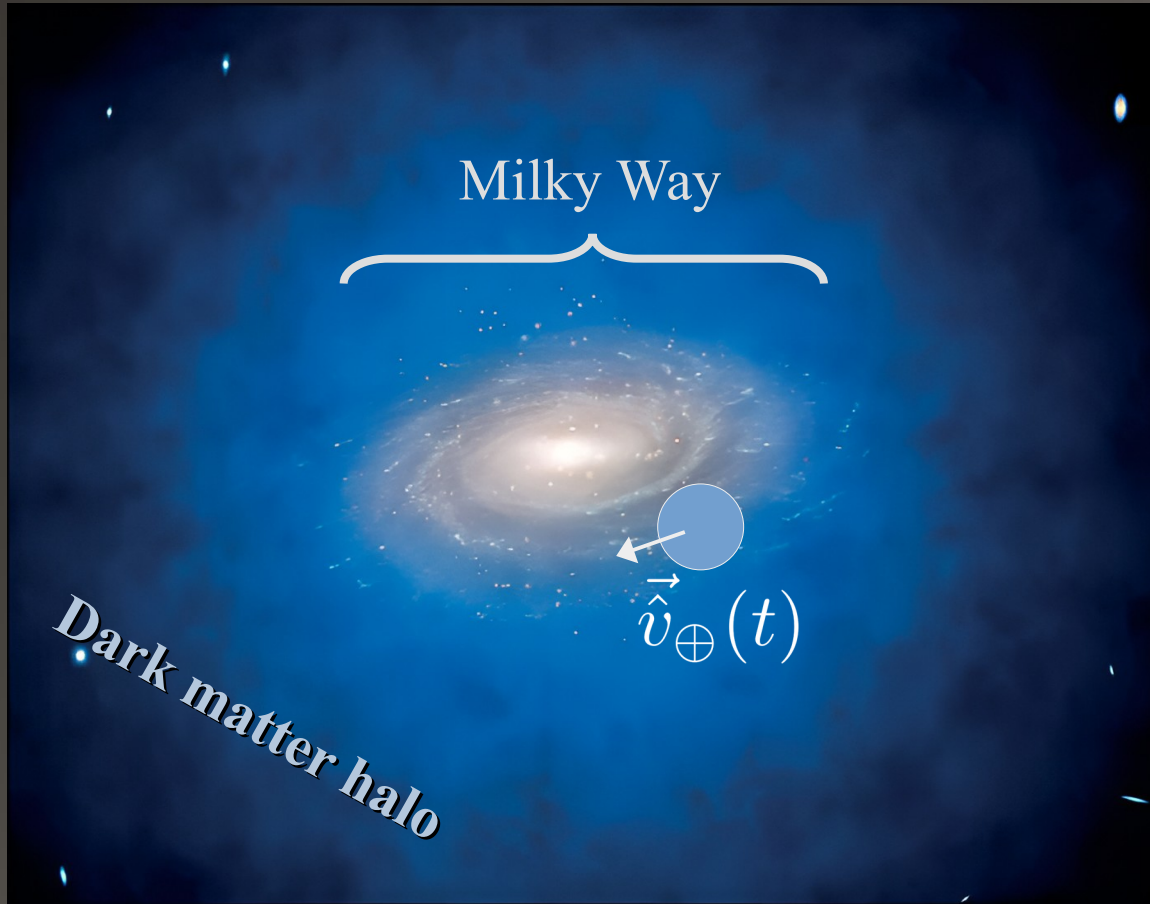
Molecular crystals have fundamentally anisotropic excitation probabilities. This leads to daily modulating signals from DM.

Option 2

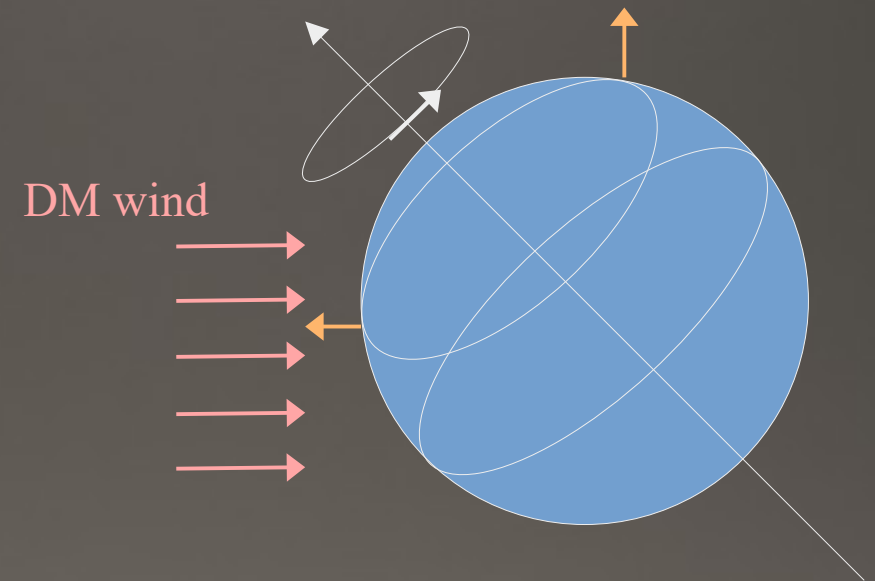
Reduce background in the emission step, i.e. selective signal generation.

Quantum dots can produce a pair of time-coincident photons following excitation.

Directional Detection



The earth experiences a dark matter “wind” in the direction of travel around the Milky Way

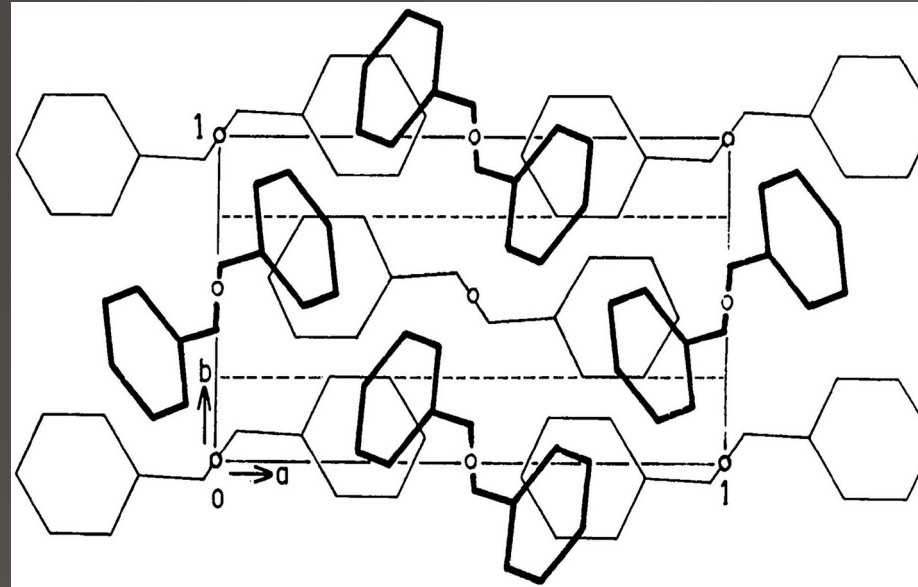


Change in relative orientation between detector and dark matter wind leads to *daily* modulation

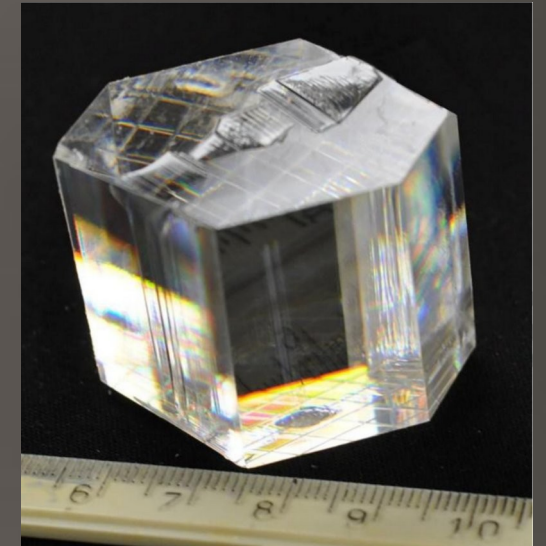
Trans-Stilbene



De-localized and planar network
of double bonds



Molecular planes oriented in
crystal lattice

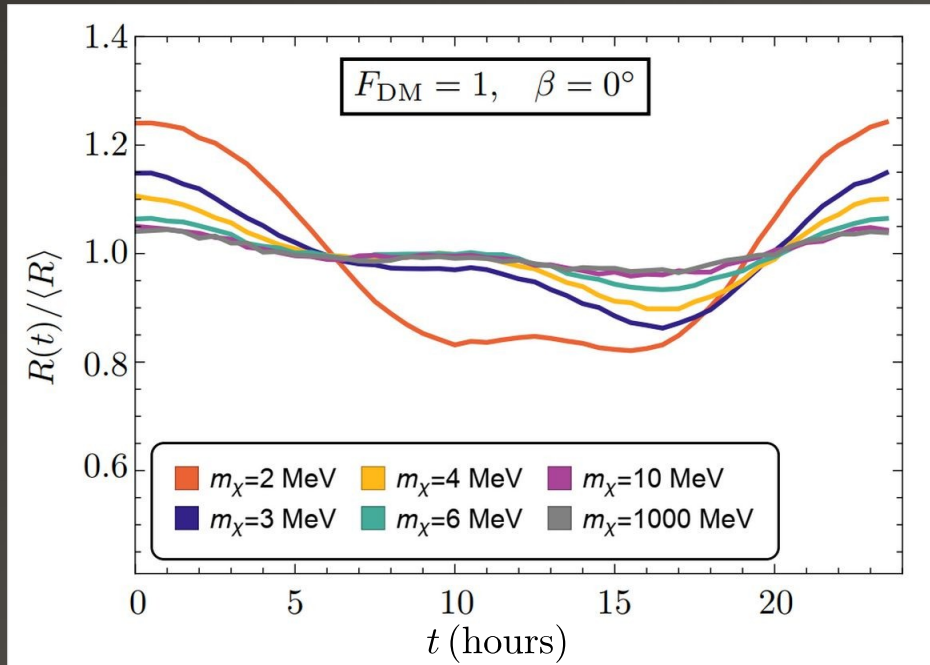


Carman, et.al. '18 (J. of Crystal Growth)

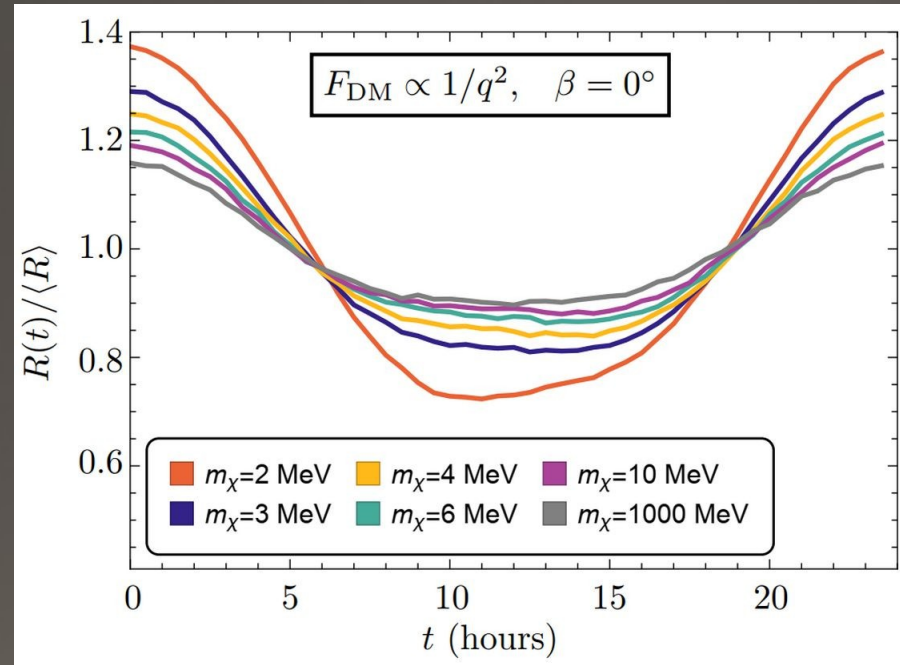
Large optical-quality crystals

Daily Modulation

(Contact interaction)



(Long-range interaction)



Predicted rate changes by up to 70% throughout the day.

That's a verifiable signal!

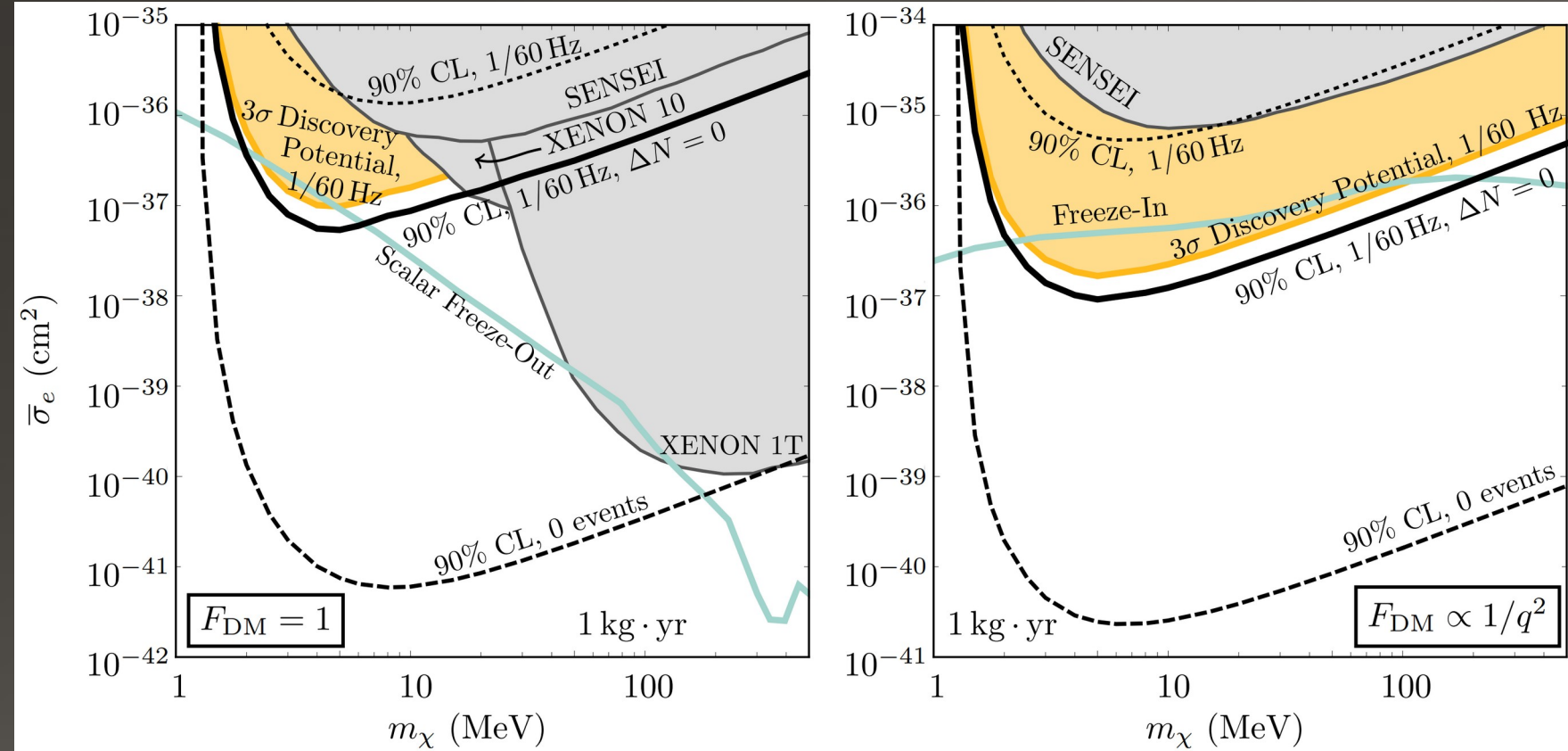
[CB, Kahn, Lillard, McDermott: 2103.08601]

Modulation amplitude remains as high as 10% even at the highest masses. This is due to the fundamental anisotropy of the molecular form factor.

Sensitivity & Reach

(Contact interaction)

(Long-range interaction)



Assuming realistic backgrounds

Exclusion w/o modulation

Discovery potential w/ mod.

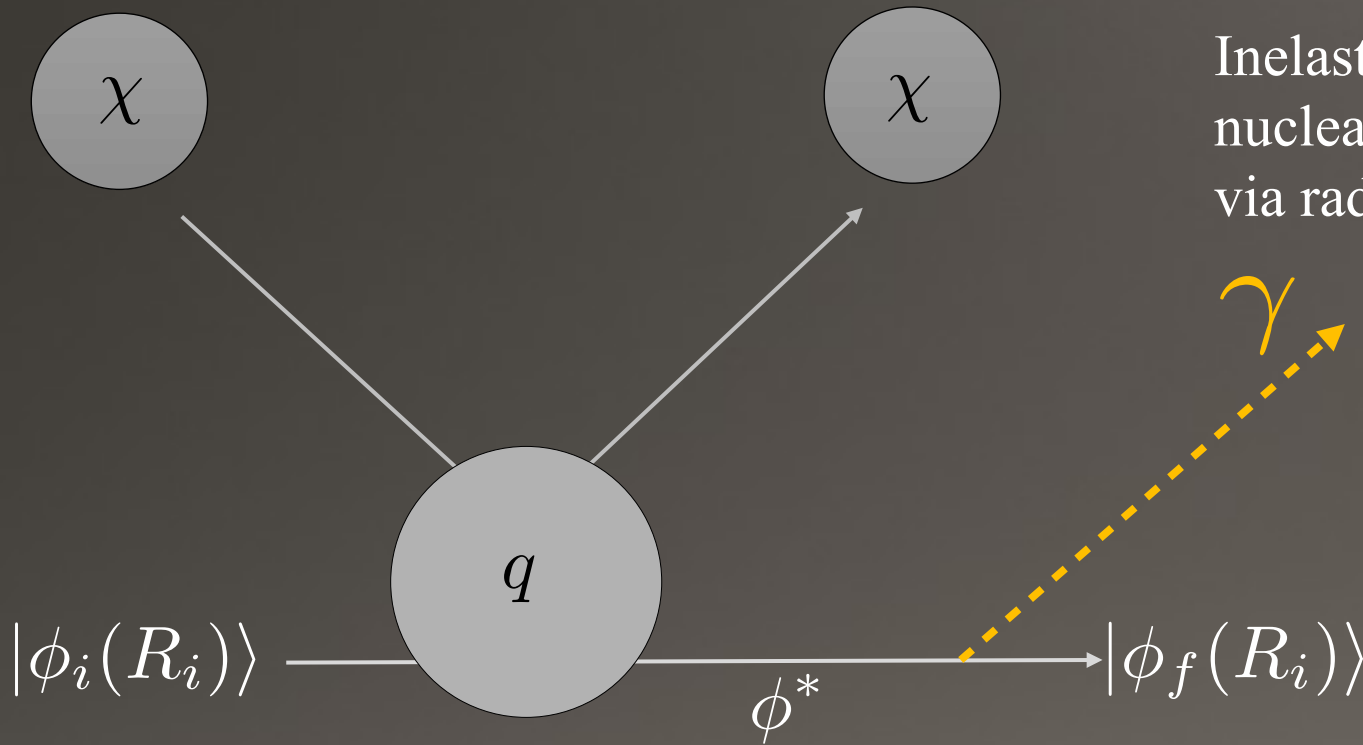
Exclusion w/ modulation

Modulating signals improve sensitivity by about two orders of magnitude and provide the potential for discovery

*1kg of t-stilbene can probably be found within a few blocks of this room

[CB, Kahn, Lillard, McDermott: 2103.08601]

Nuclear Recoil: Photon Signal

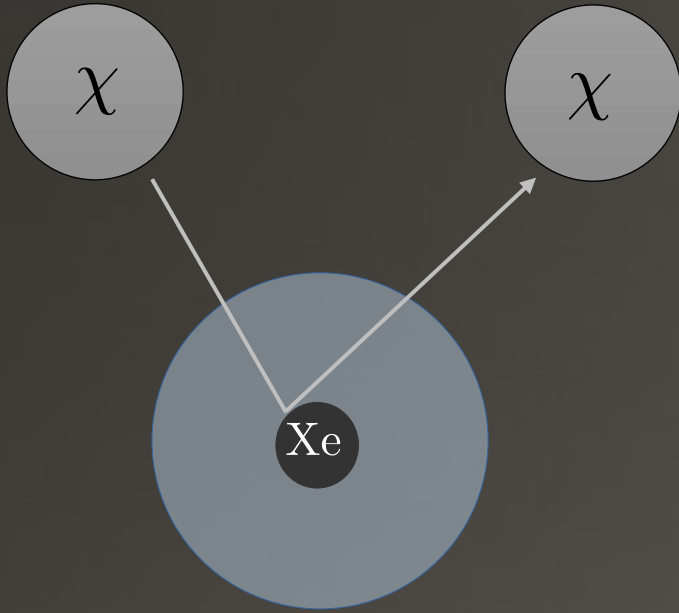


Inelastic scattering or bosonic absorption on nuclear states leads to an excitation that decays via radiative emission.

Nuclear scattering

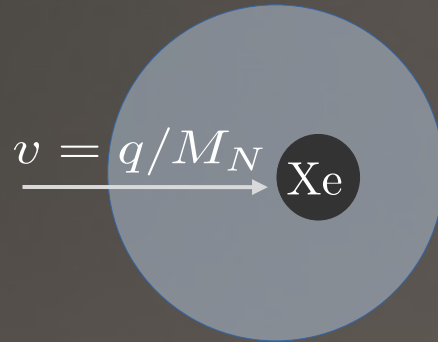
$$\Delta E \sim \mathcal{O}(\text{few eV}) \left(\frac{m_\chi}{100 \text{ MeV}} \right)^2 \left(\frac{m_N}{130 \text{ GeV}} \right)^{-1}$$

Ionizing through nuclear recoil: Atoms

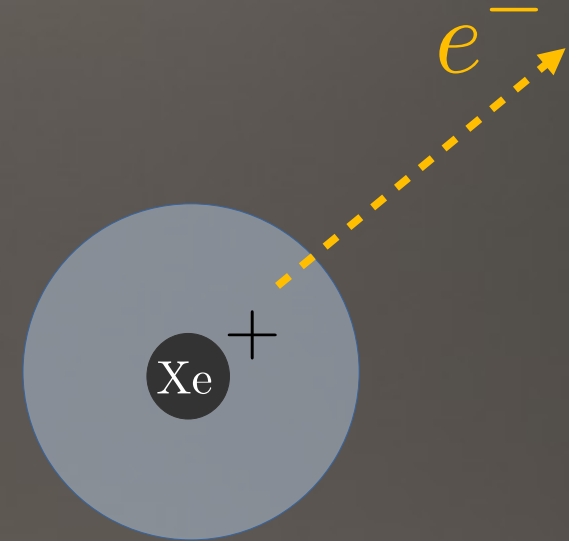


Initial nuclear recoil

$$|\psi_i\rangle \sim e^{i \frac{m_e}{M_N} \vec{q} \cdot \vec{r}} \psi_{\text{AO}}(r_\beta)$$



Nucleus recoils faster than motion of electrons



Electronic transition to ionized state

$$f_{i \rightarrow f} \approx \frac{m_e}{M_N} \vec{q} \cdot \langle \vec{r} \rangle_{i \rightarrow f}$$

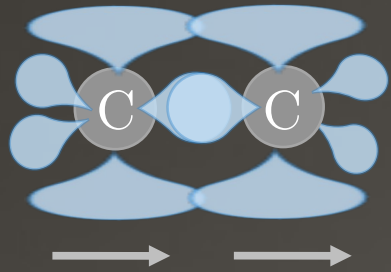
The Migdal effect in atoms has been invoked in e.g. Xenon to extend the sensitivity of noble liquid detectors to lower masses.

Migdal transition probability is suppressed by kinematic mis-match.

The Molecular Migdal Effect(s)

Center of mass recoil (CMR) effect

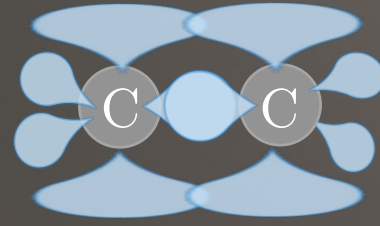
Caused by center of mass motion



COM recoil effect is the molecular analog of the semiclassical Migdal effect

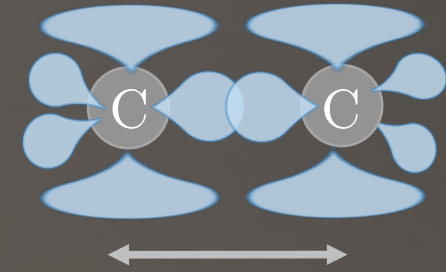
$$P_{CMR} \sim \frac{m_e}{M_{mol}}$$

Suppressed by kinematic factor due to moving the whole molecule.



Non-adiabatic coupling (NAC) effect

Caused by relative motion



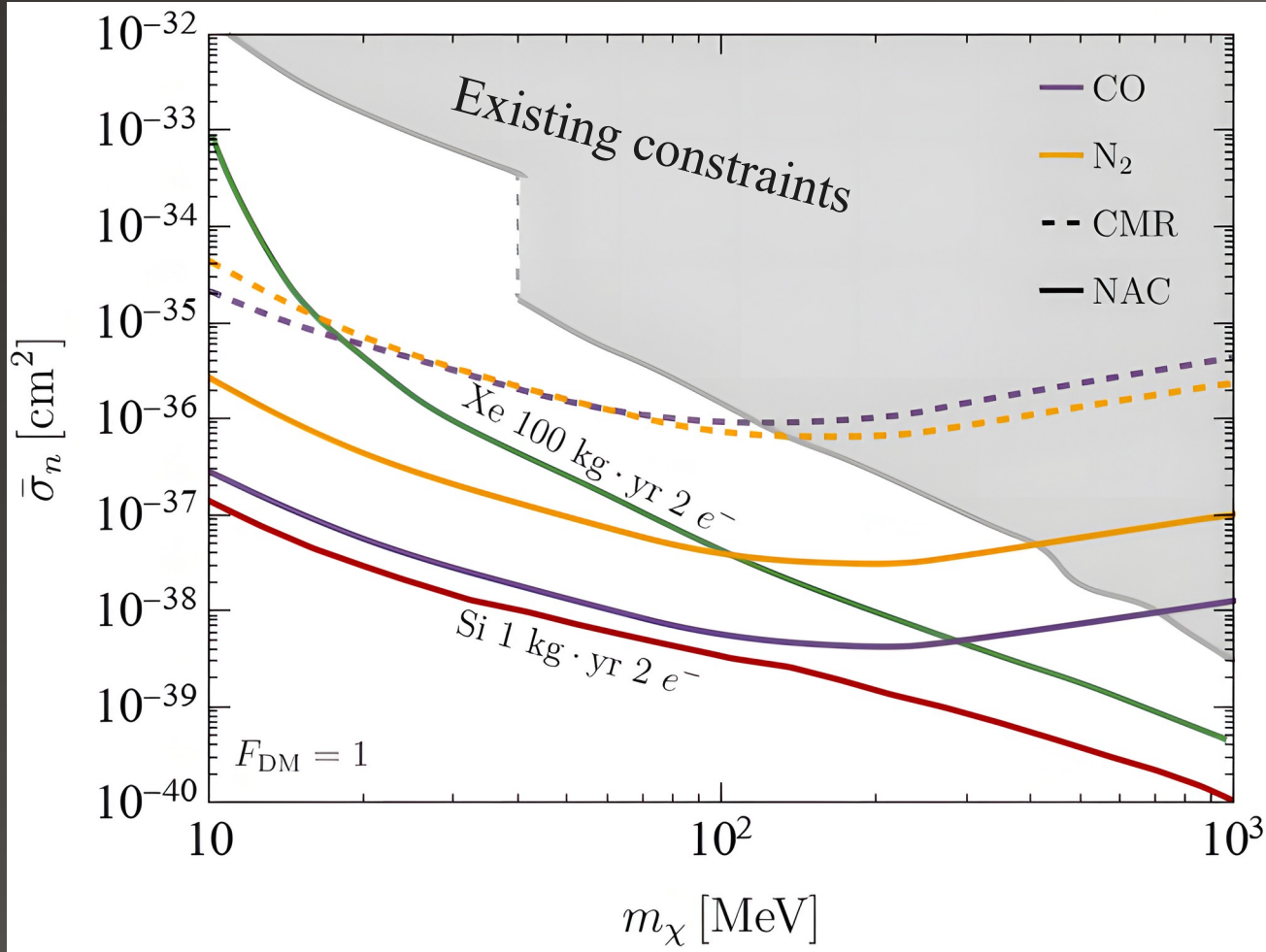
NAC caused by effects beyond Born-Oppenheimer approximation

$$P_{NAC} \sim \frac{m_e}{M_N}$$

Suppressed by kinematic factor due to moving a single atom.

The Molecular Migdal Effect(s)

(Contact interaction)



Si rate is calculated using the *CMR*-equivalent Migdal effect. Is there an *NAC*-equivalent in Si?

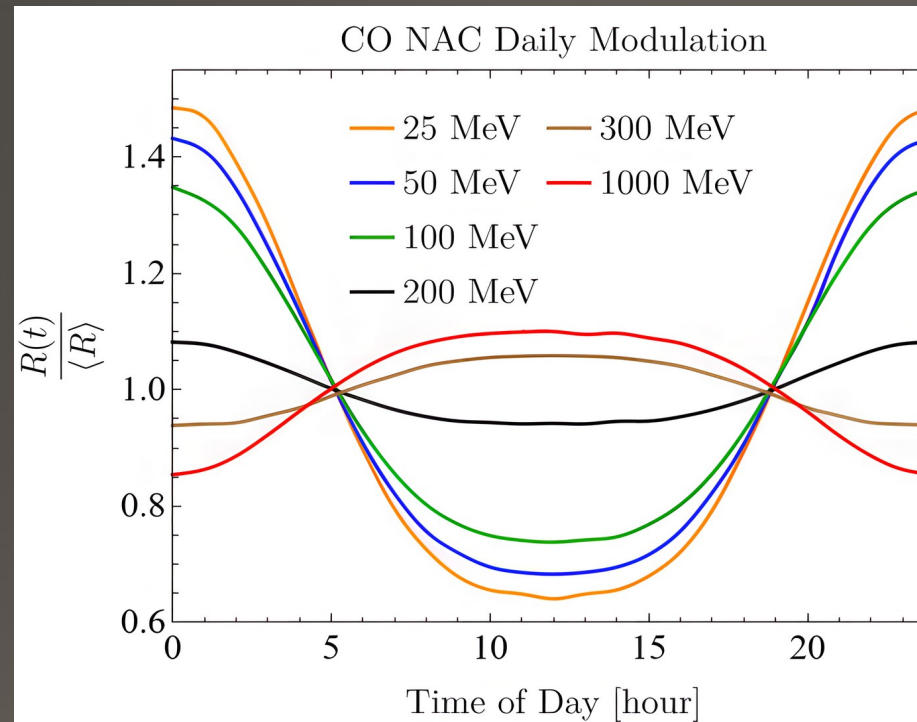
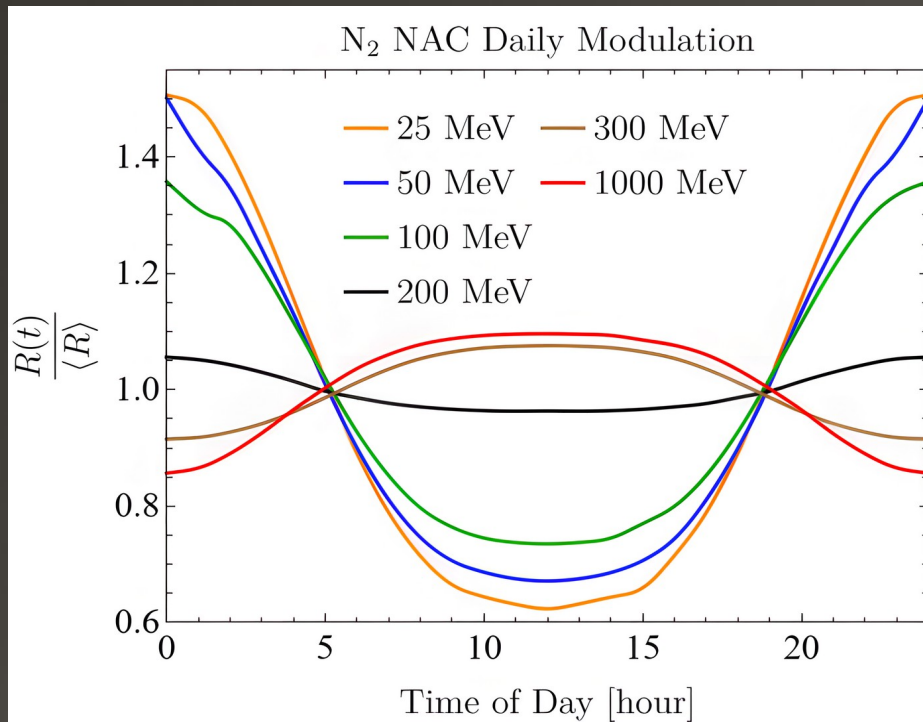
← *Center of mass recoil* effect is predicted to be subdominant at all masses.

← *Non-adiabatic coupling* effect is predicted to dominate due to favorable kinematic factor.

Simplest molecular models already competitive. Is there an optimal molecular target?

[CB, Harris, Kahn, Lillard, Perez-Rios: 2208.09002]

Directional Molecular Migdal Effect



Predicted rate changes by up to 80% throughout the day.

The daily modulation phase is mass dependent.

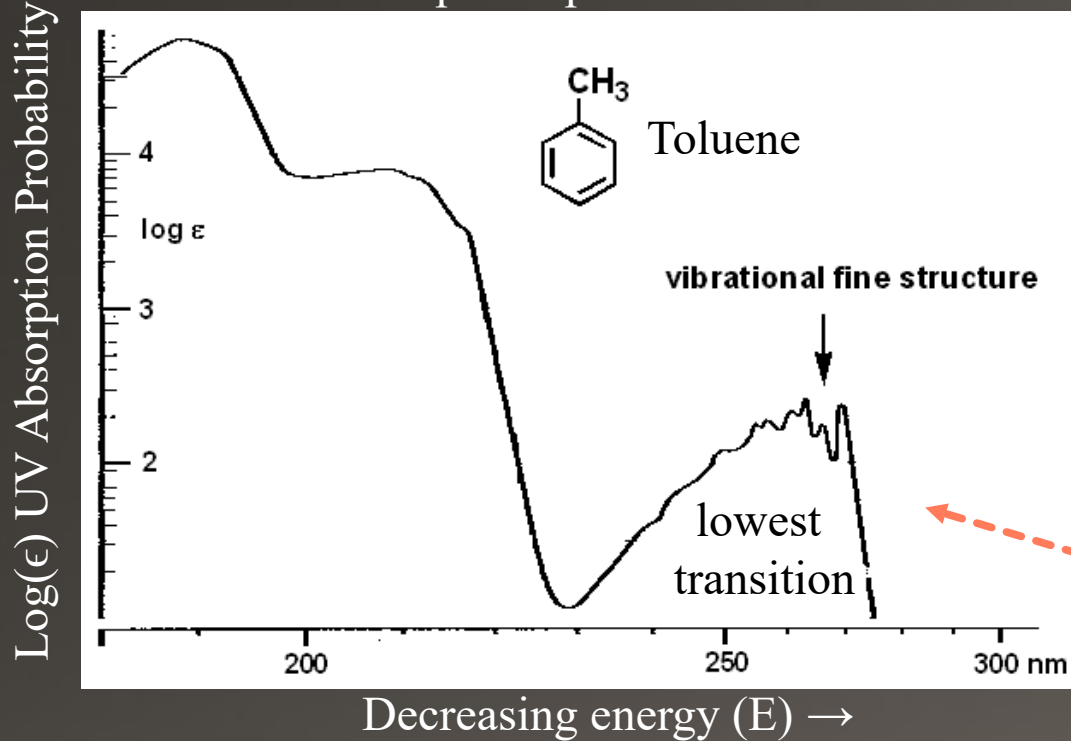
[CB, Harris, Kahn, Lillard, Perez-Rios: 2208.09002]

Persistent daily modulation at large dark matter mass is generically predicted for the molecular Migdal effects.

We predict that the same class of molecules that make good directional detectors for electron scattering will also be ideal for nuclear scattering because of the directional molecular Migdal effects.

Finding optimal targets for NAC

UV Absorption spectrum of toluene



Non-adiabatic form factor is asking about how the electrons respond to nuclear deformation.

$$f_{e,NAC} \sim \langle \psi_f | \nabla_R | \psi_i(r) \rangle$$

Recall that photon absorption is proportional to the transition dipole moment.

$$\epsilon \sim \langle \Psi_f | \vec{r} | \Psi_i \rangle = 0$$

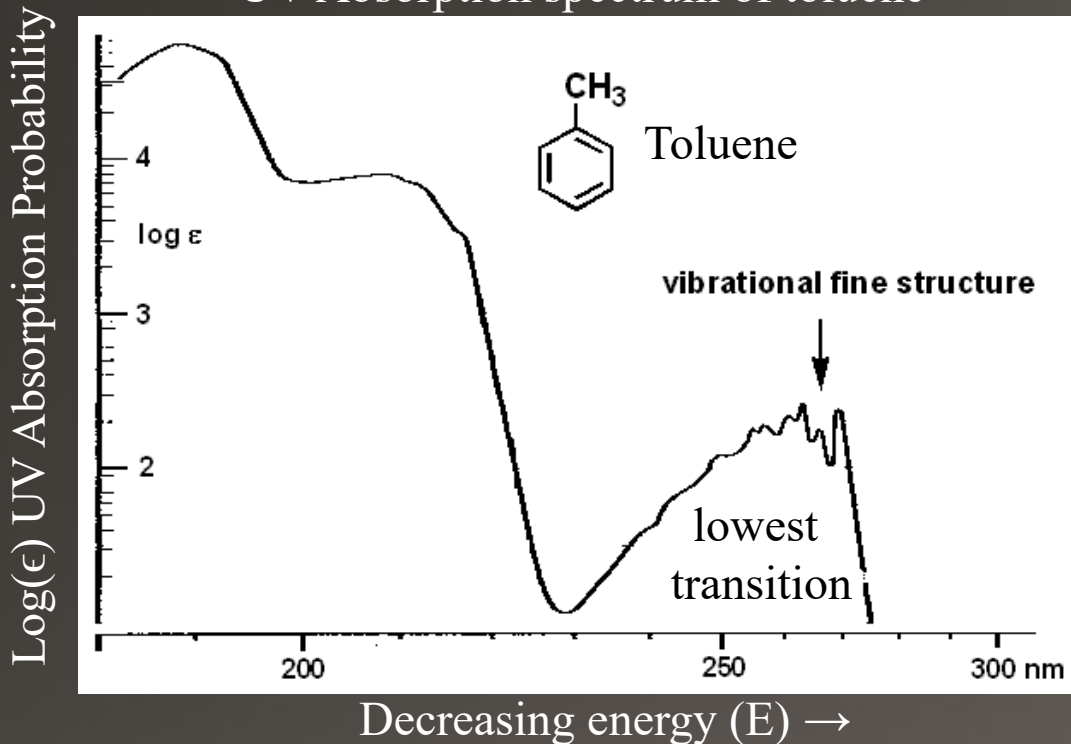
That's classically forbidden by symmetry

Molecules with vanishing transition dipole moments are classically forbidden from absorbing. However, a deformation in the molecular structure can generate a dipole, i.e. a measurable NAC-induced absorption!

$$\epsilon \sim \langle \psi_f(r; R) | \vec{r} | \psi_i(r; R) \rangle |_{R \neq R_0} \neq 0$$

Finding optimal targets

UV Absorption spectrum of toluene



Problem: Chemical space is unreasonably large

How many molecules can be made with only C, O, N, F, & H?

9 atoms: 100s of Thousands (DFT Computable)

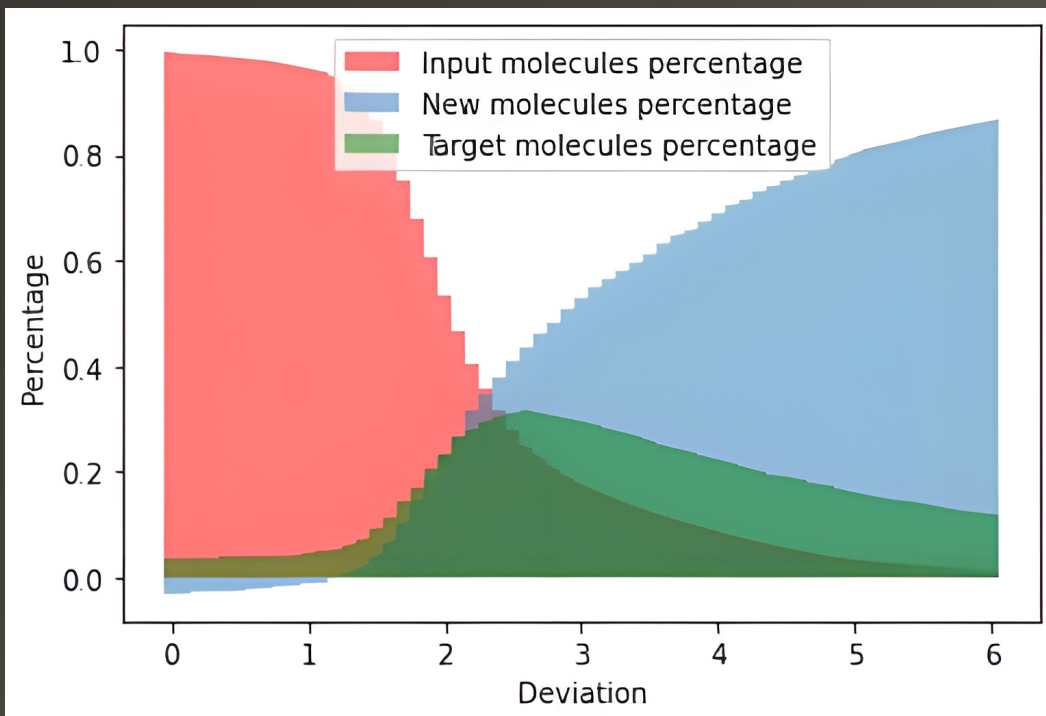
30 atoms: 100s of Billions (Intractable)

toluene has 15, xylene has 18, t-stilbene has 26

We need a method to:

1. Look for favorable properties - *cheminformatics*
2. extra(intra)polate onto new molecules – *machine learning*

ML for DM Direct Detection



Machine learning can do both of these

How many molecules can be made with only C, O, N, F, & H?

9 atoms: 100s of Thousands (Complete dataset— QM9)

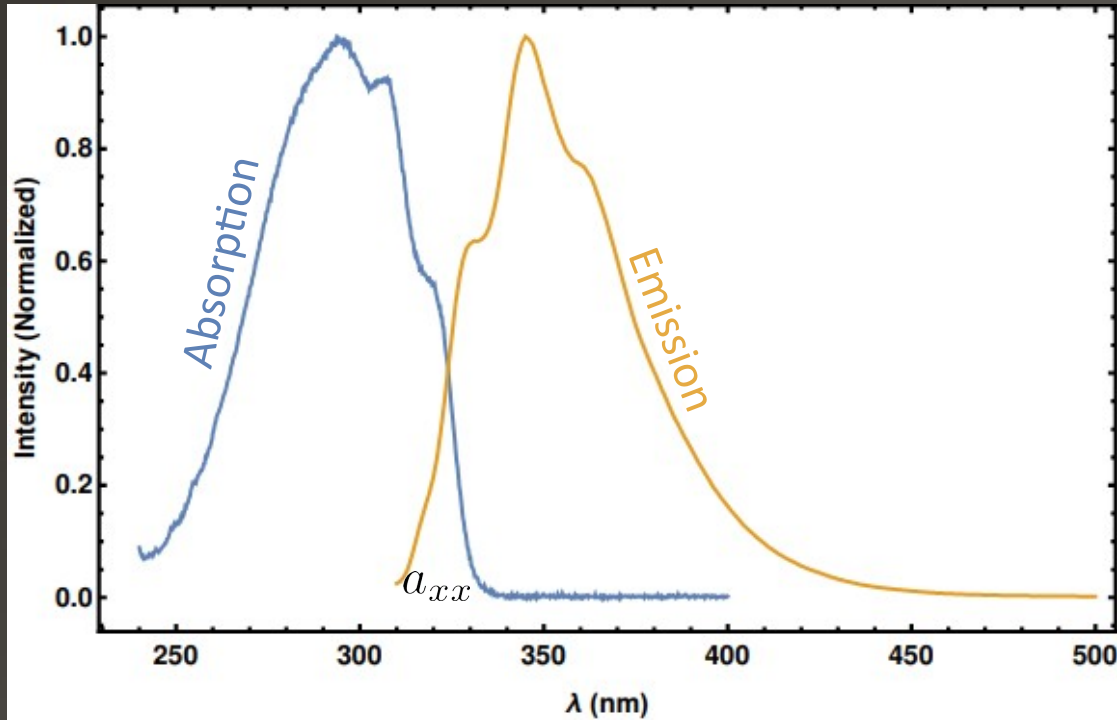
30 atoms: 100s of Billions (Sparse data)

Validate on QM9 then apply interpolator to larger set

Method:

1. Learn the latent space of molecules → Property prediction
2. Generate new molecules by optimizing for properties in lower dimensional space.

Fluorescence with DM Works



Now what we need is:

Lower background

Option 1

Reduce background in the absorption step, i.e. selective excitation.

Molecular crystals have fundamentally anisotropic excitation probabilities. This leads to daily modulating signals from DM.

Option 2

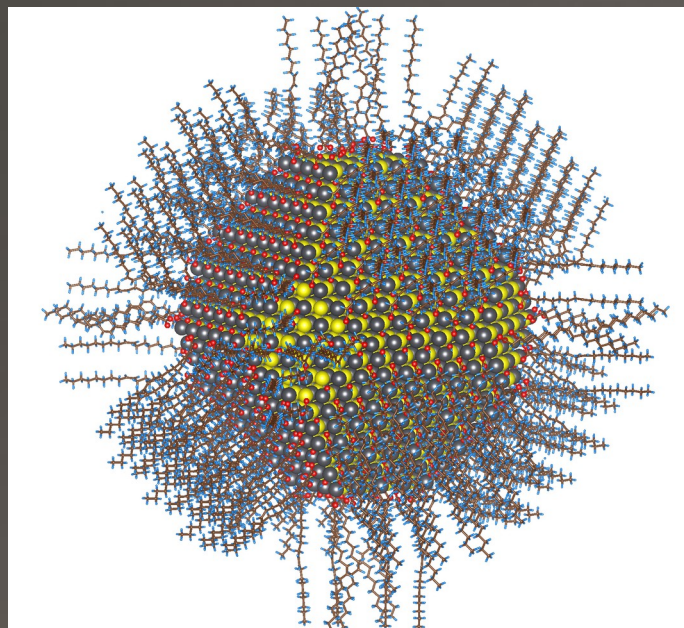
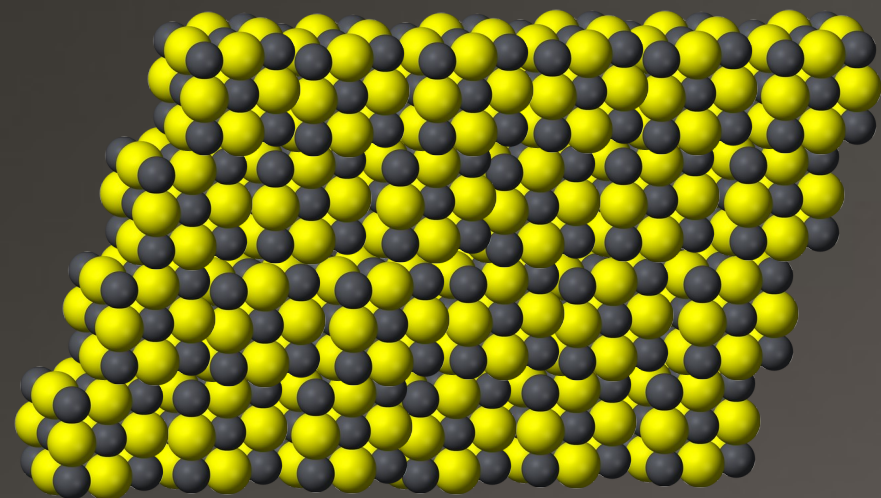
Reduce background in the emission step, i.e. selective signal generation.

Quantum dots can produce a pair of time-coincident photons following excitation.

What are Quantum Dots?

Quantum confinement affects the long-wavelength physics

Quantum confinement



$R \rightarrow \infty \text{ nm}$

$R \sim \mathcal{O}(\text{few nm})$

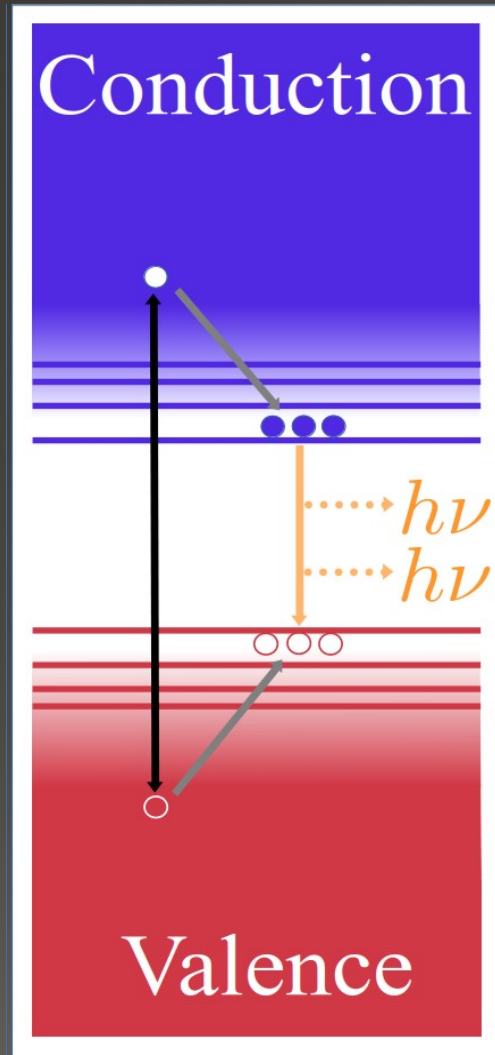
$$|\psi_i\rangle \sim u_{\text{Bloch}}(r) e^{ik \cdot r}$$

$$|\psi_i\rangle \sim u_{\text{Bloch}}(r) \psi_{\text{bound}}(r)$$

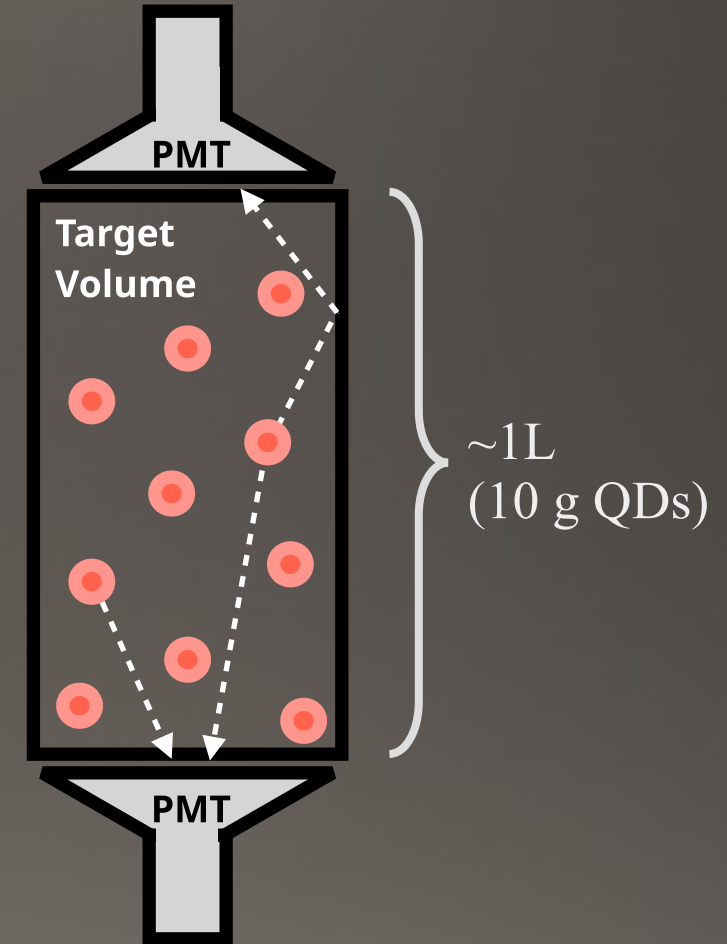
$E(k)$

Zherebetsky et al., Science 344, 1380 (2014)

Quantum Dots



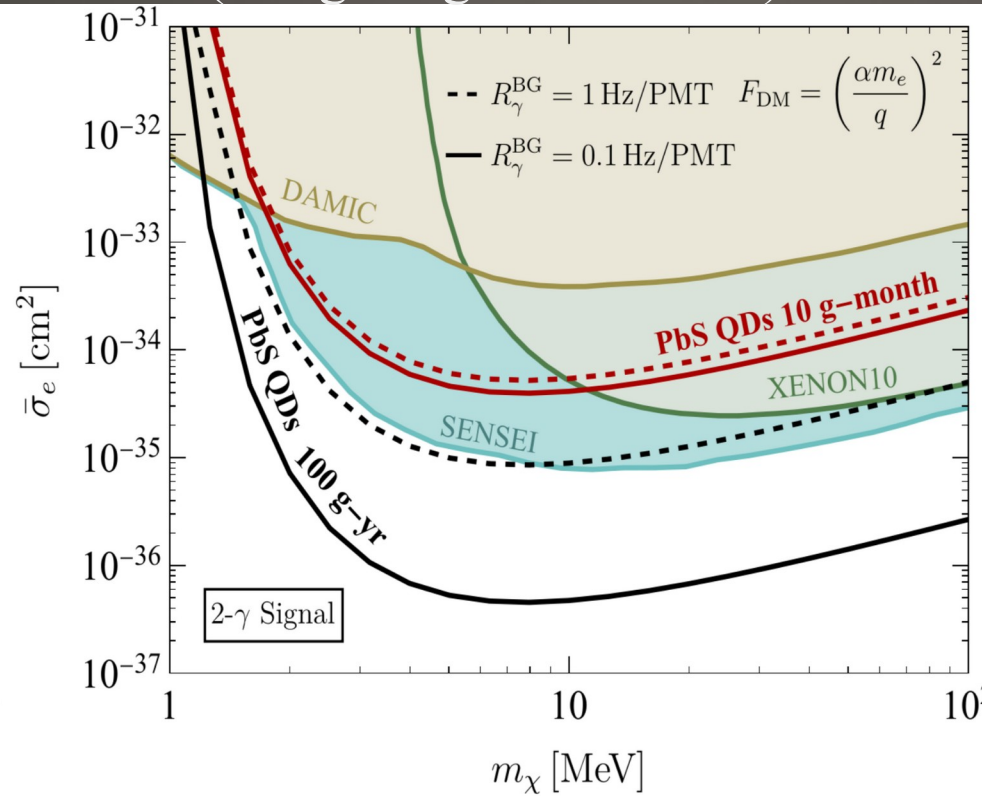
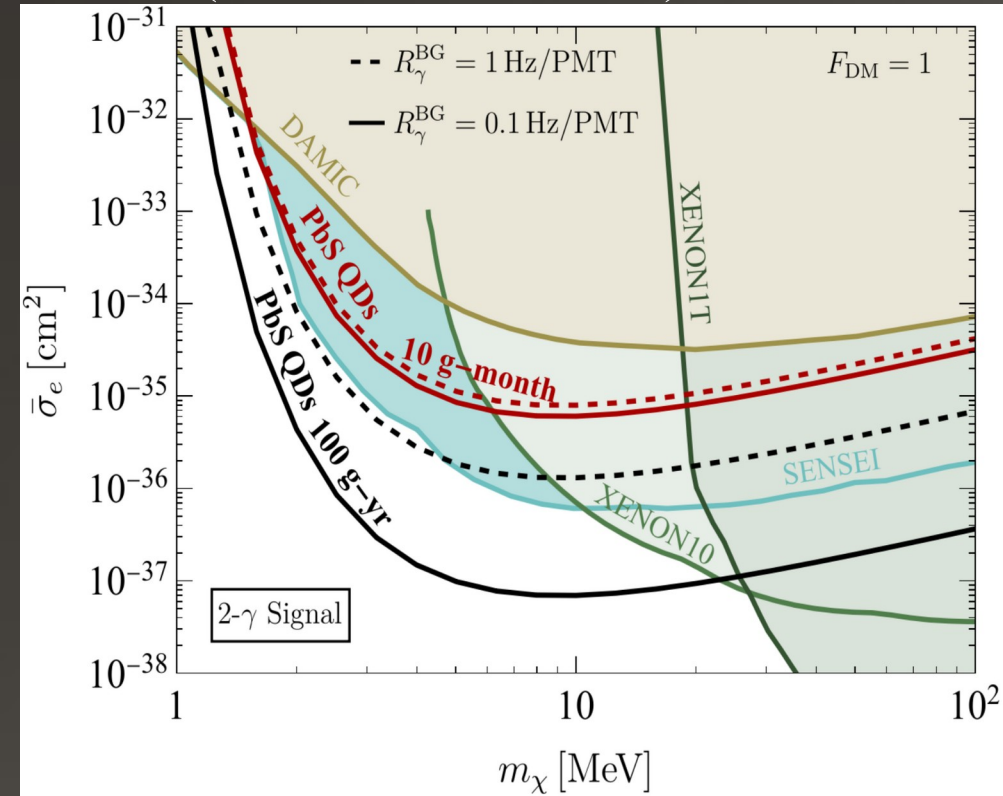
- **Absorption:** Creation of a “hot” exciton – an electron/hole pair with energy significantly larger than the bandgap
- **Non-Radiative Transition:** Multi-exciton generation when energy is greater than twice the bandgap creates several band-edge excitons.
- **Emission:** Radiative recombination of several band-edge excitons producing several coincident photons



PbS Quantum Dots

(Contact interaction)

(Long-range interaction)



Essentially background free @ this scale

[CB, Essig, Fernandez-Serra, Ramani, Slone: 2208.05967]

Assuming a realistic dark rate for the photodetectors, QD-based detectors using existing technology would be deployed and easily scaled to overtake existing limits.

Deployment

LETTER OF INTENT:

QUAntum dot **D**ark matter **R**ecoil detection with **A**balone
photosensors (QUADRA)

Carlos Blanco^{1,2}, Jan Conrad², Rouven Essig³, Alfredo Davide Ferella⁵, Tim Linden², Jörn
Mahlstedt², and Val Zwiller⁴

¹*Department of Physics, Princeton University, Princeton, NJ 08544, USA*

²*Stockholm University and The Oskar Klein Centre for Cosmoparticle Physics, Alba Nova,
10691 Stockholm, Sweden*

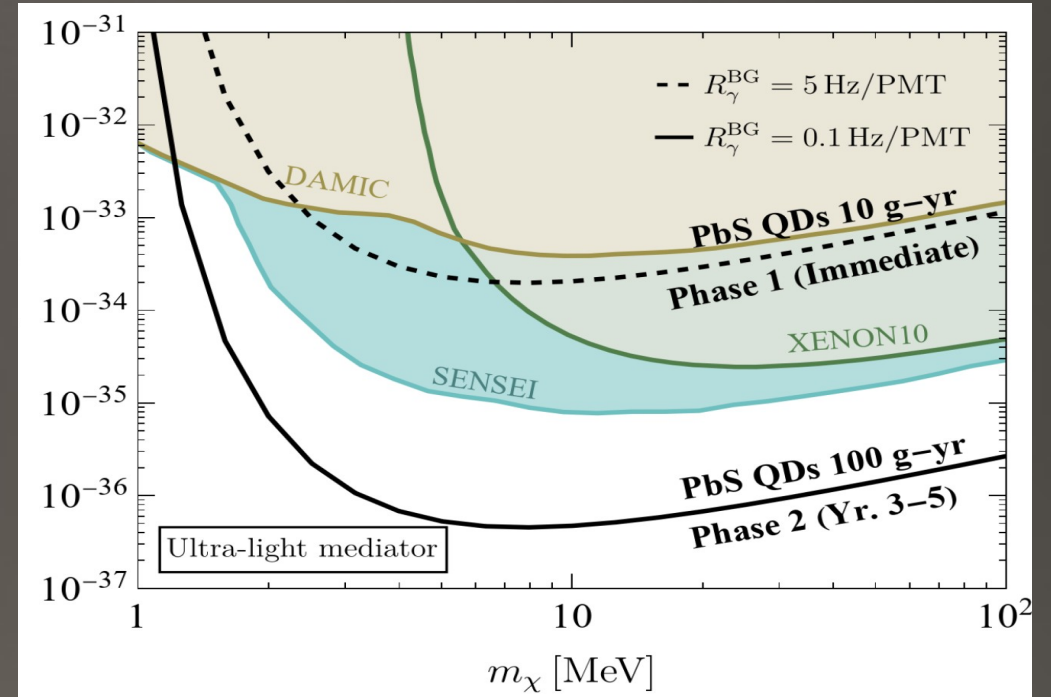
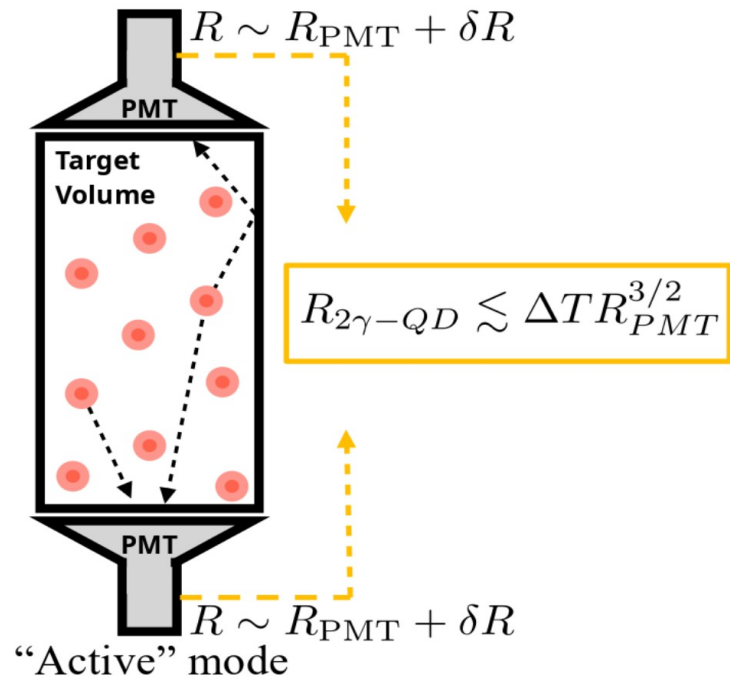
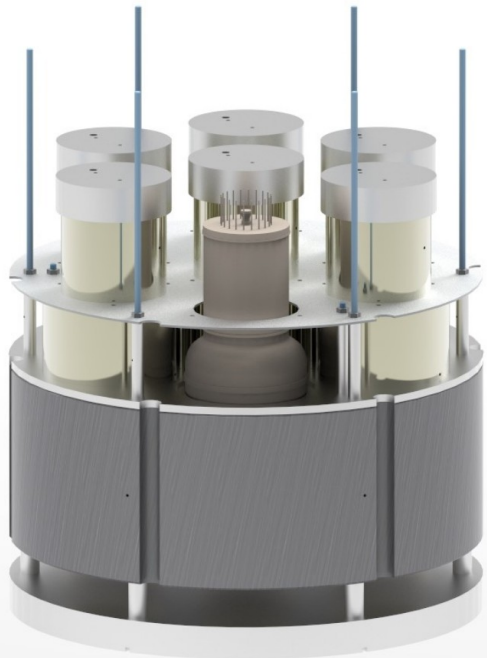
³*C. N. Yang Institute for Theoretical Physics, Stony Brook University, USA*

⁴*Department of Applied Physics, Royal Institute of Technology, Roslagstullsbacken 21, 114
21 Stockholm, Sweden*

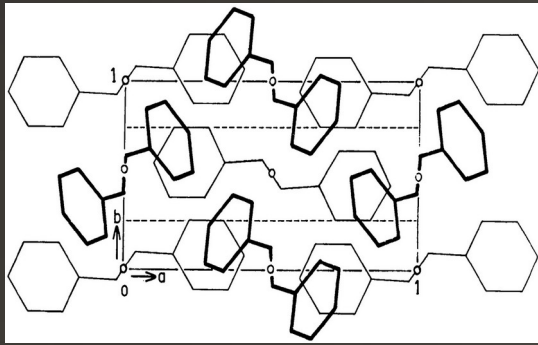
⁵*Department of Physics and Chemistry, University of L'Aquila, 67100 L'Aquila, Italy and
INFN-Laboratori Nazionali del Gran Sasso and Gran Sasso Science Institute, 67100
L'Aquila, Italy*

October 31, 2022

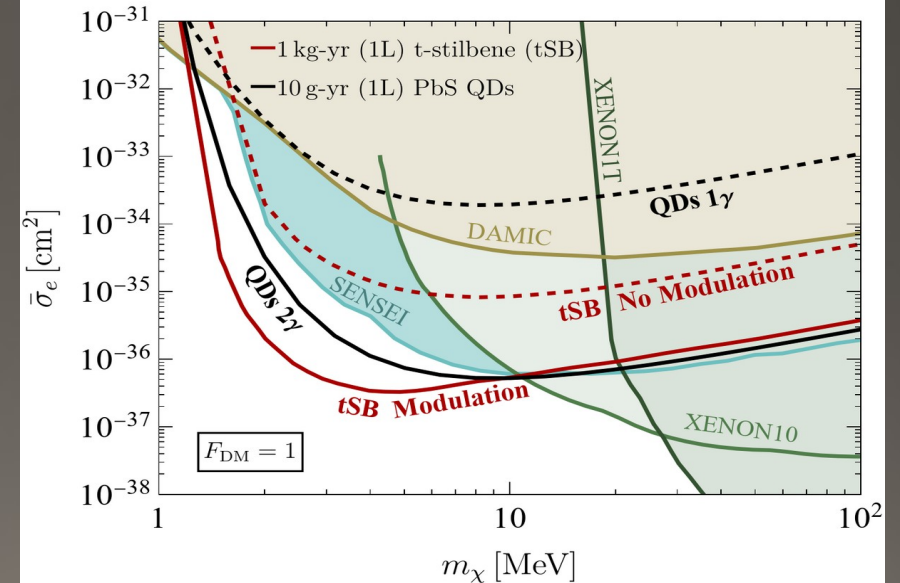
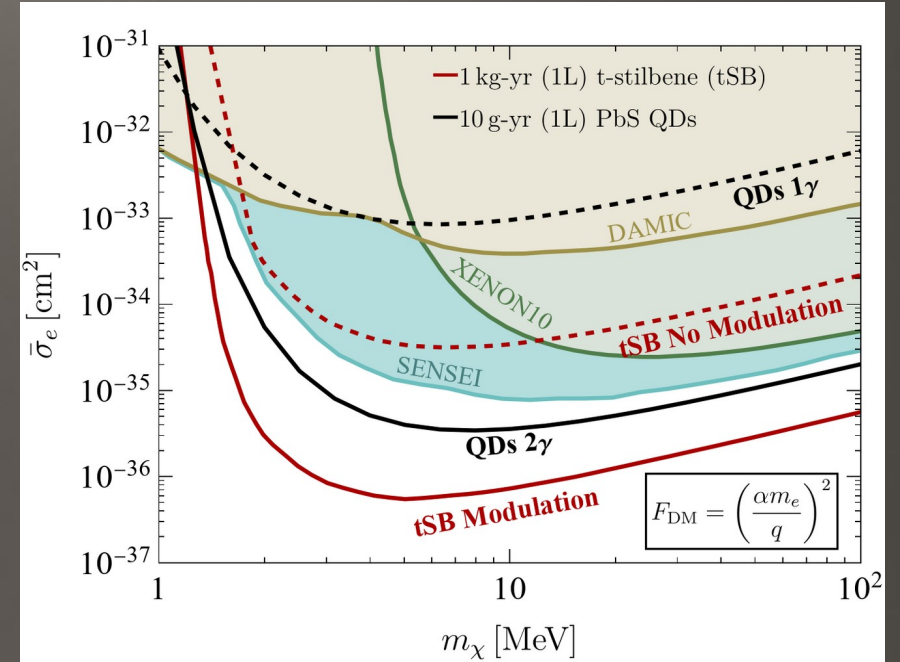
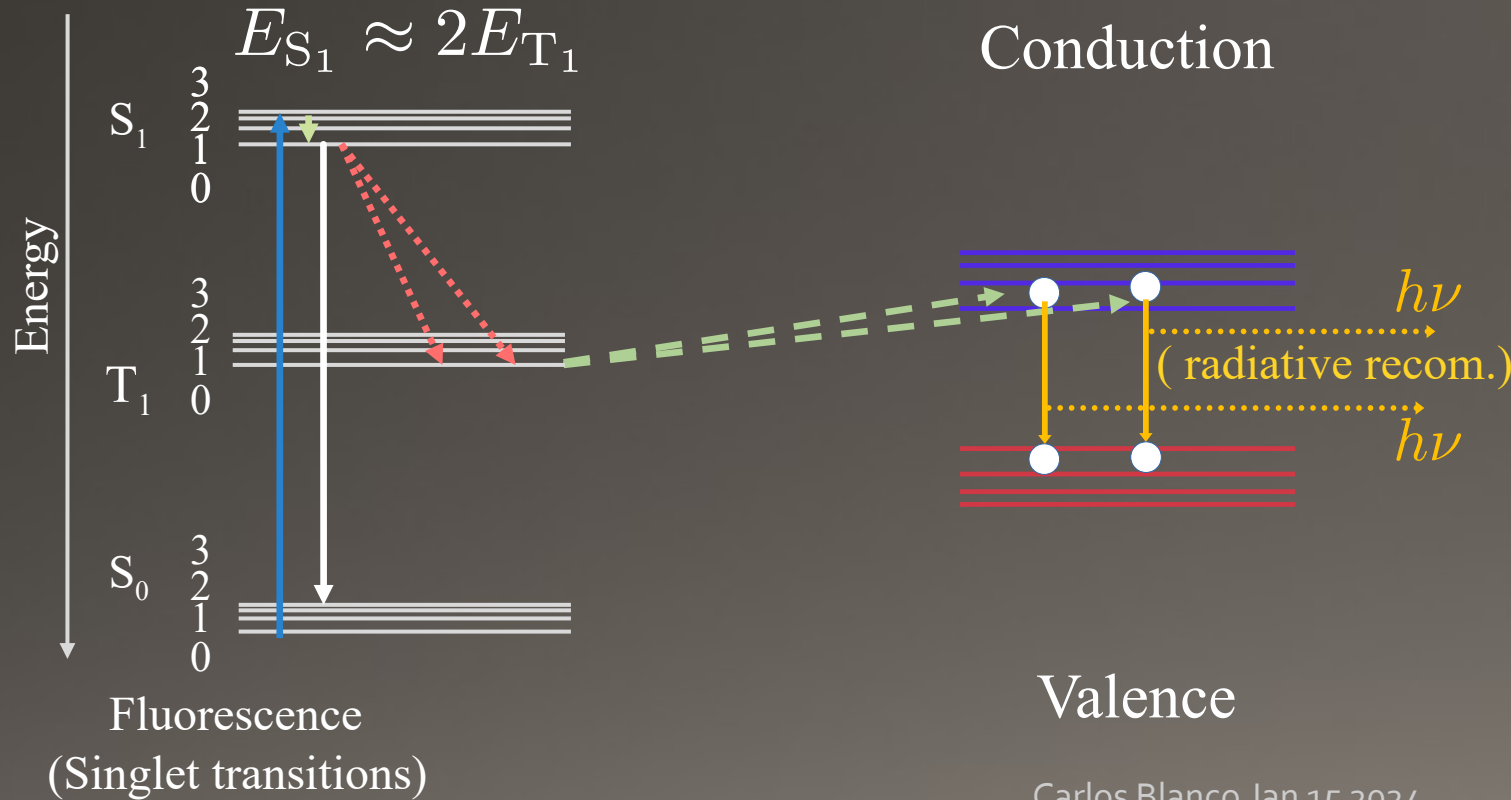
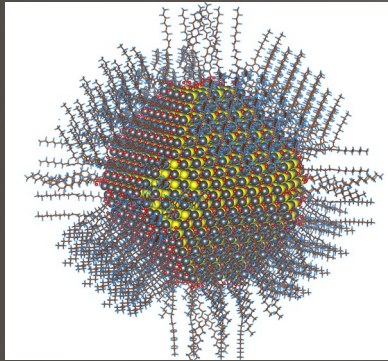
Deployment



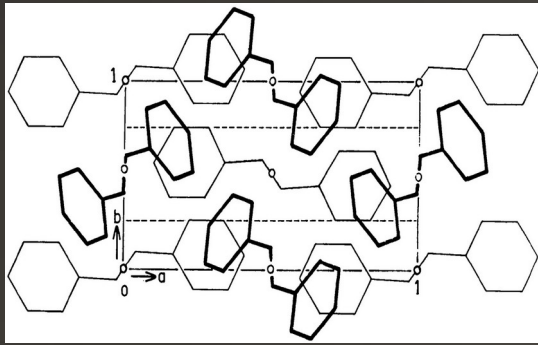
Hybrid Detectors



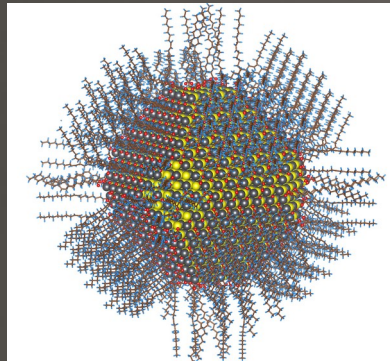
(Charge Transfer)



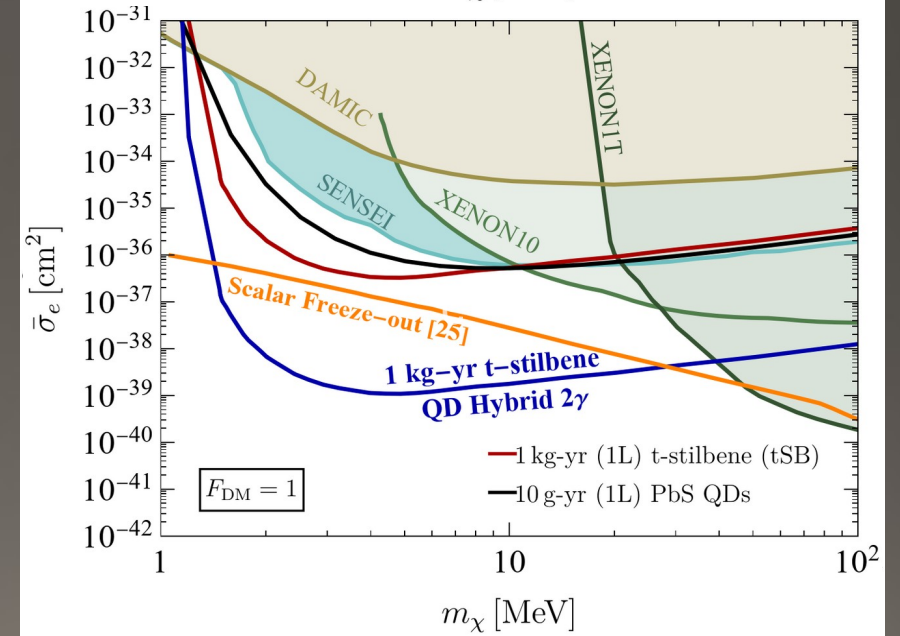
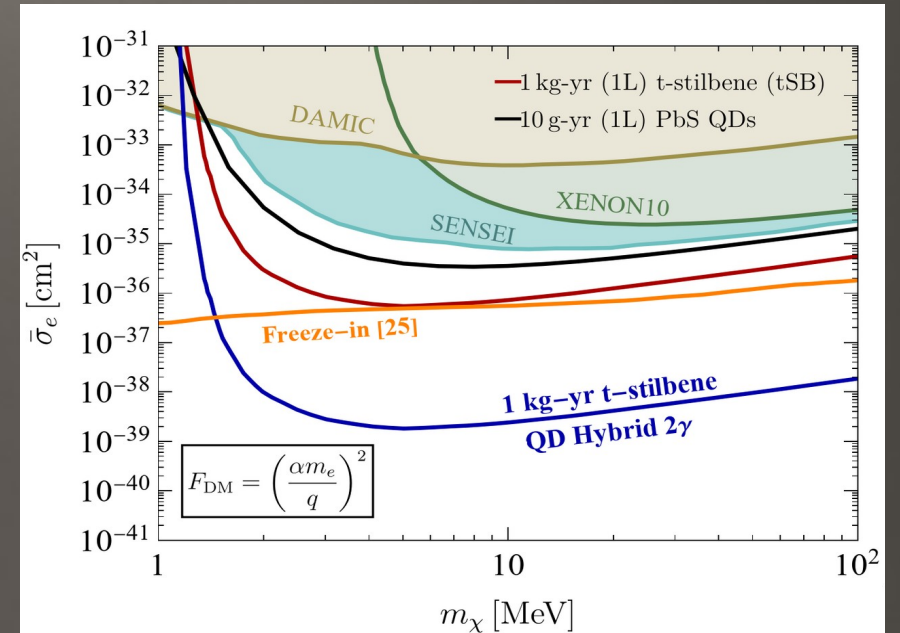
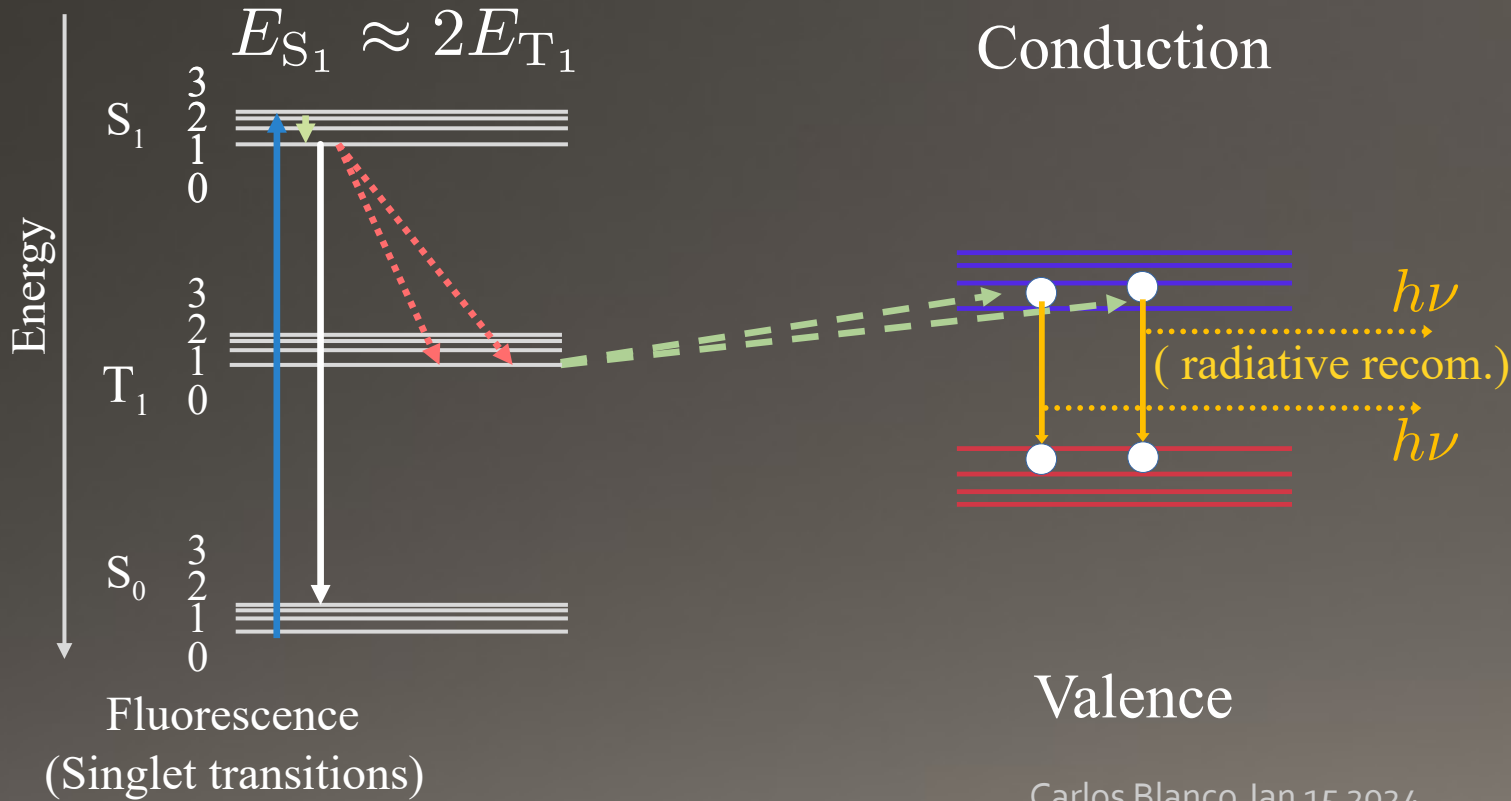
Hybrid Detectors



(Charge Transfer)



Conduction



Conclusions

- 1) We have done an extremely effective job looking for WIMPs, now we must look beyond.
- 2) By developing the formalism that describes the interaction between dark matter and molecules or nano-materials, we can propose detection strategies capable of *delving deep* and *searching wide* across the dark matter parameter space.
- 4) This remains one of the few ways to probe high-energy physics at the bench-top scale.
- 5) Future hybrid methods may bring together both strategies giving multiplicative improvements to sensitivity.

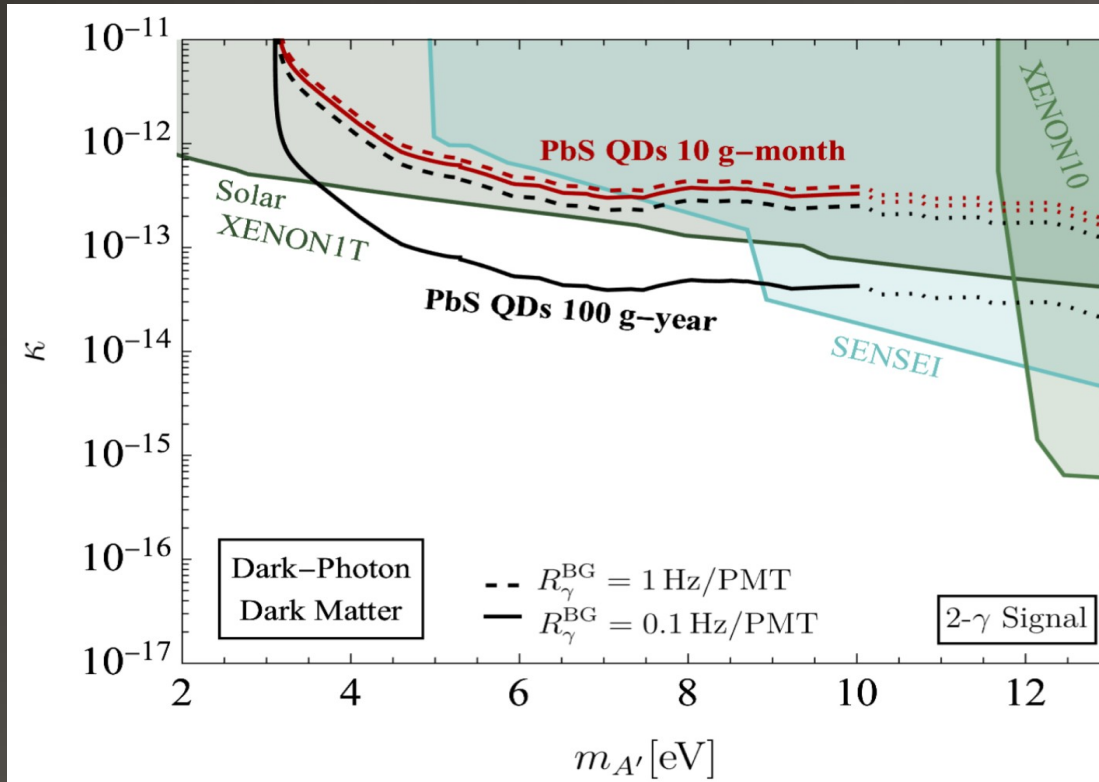
Acknowledgements

- Collaborators & colleagues: Yoni Kahn, Ben Lillard, Juan Collar, Jesus Perez-Rios, Rouven Essig, Hari Ramani, Oren Slone, Dan Baxter, Marivi Fernandez-Serra, Sam McDermott, Ian Harris (In no particular order)
- The work of C.B. was supported in part by NASA through the NASA Hubble Fellowship Program grant HST-HF2-51451.001-A awarded by the Space Telescope Science Institute, which is operated by the Association of Universities for Research in Astronomy, Inc., for NASA, under contract NAS5-26555 as well as by the European Research Council under grant 742104.



PbS QDs

Dark photon kinetic coupling



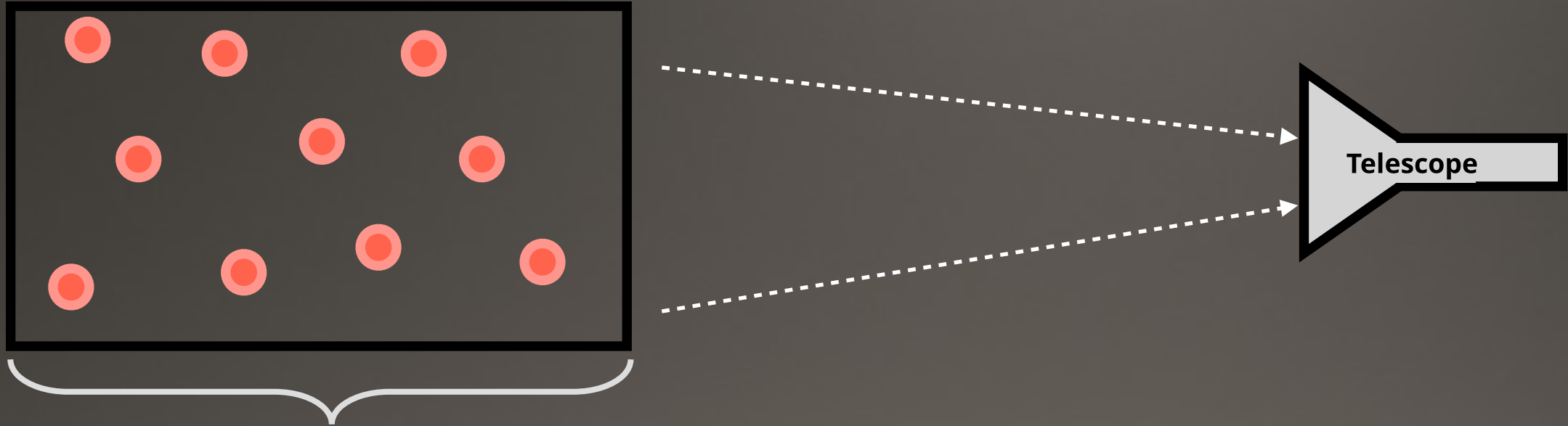
[CB, Essig, Fernandez-Serra, Ramani, Slone: 2208.05967]

In the case of eV-scale dark photon absorption, we can use existing *data* to predict the sensitivity of QD-based detectors.

Key conclusions of QD analysis

- 1) The interaction rate in a semiconductor generated by DM is the same if the semiconductor is *monolithic* or *nanoscopically* disperse.
- 2) In a QD-based experiment, the readout is independent of the target.
- 3) The signal can be tuned through control of quantum confinement.

Beyond direct detection



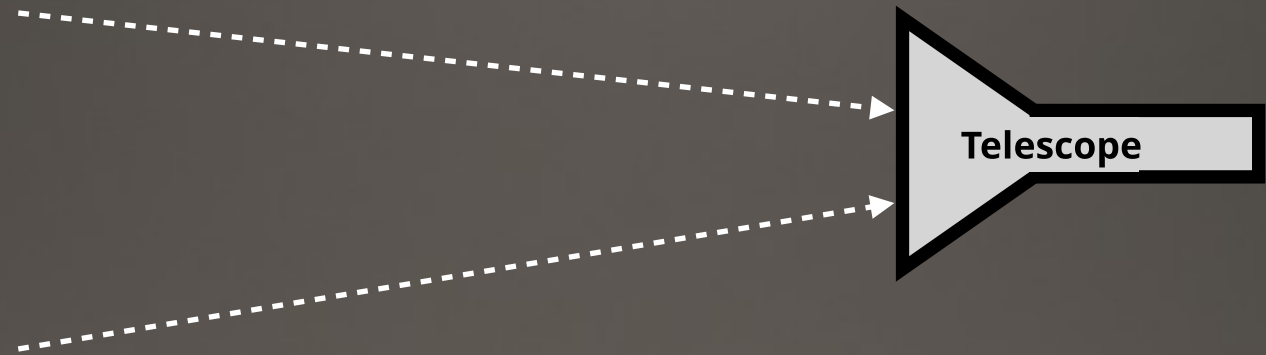
Astrophysical volume of molecules

We can use the same theoretical techniques that we've developed to predict rates in *astrophysical* objects

Beyond direct detection



Cold molecular cloud



We can use the same theoretical techniques that I've developed to predict rates in detectors to predict rates in *astrophysical* objects

Dark matter in Molecular Clouds



Very dense and cold molecular clouds are almost entirely opaque.

$$n_{\text{H}_2} \sim O(10^2)\text{cm}^{-3}$$

Ionization from CR produces ionization fraction: ζ^{H_2}

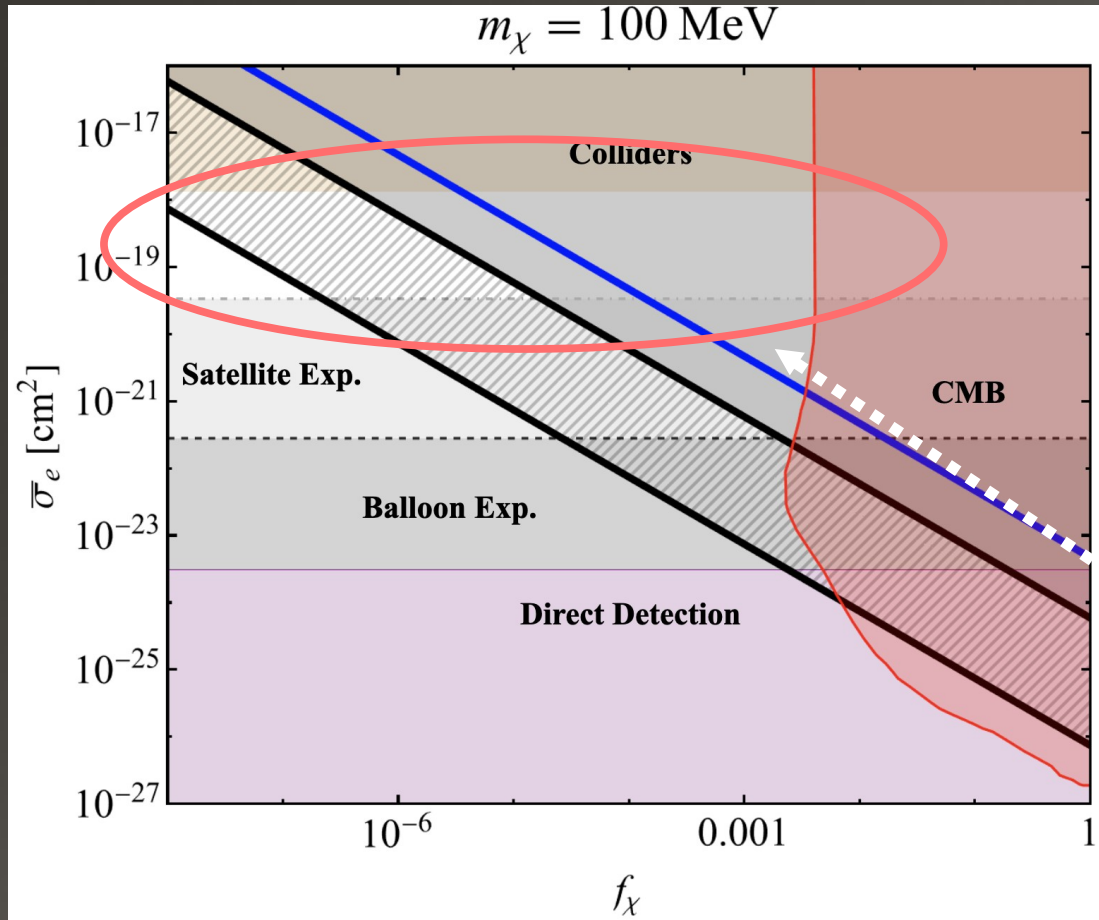


This is well measured through astro-spectroscopy of tracer molecules (line intensity measurements)

However, DM annihilation into ionizing SM particles can also produce ionized fraction

$$\zeta_i^{\text{H}_2} = 2\pi \int \frac{dN_i}{dE}(E) \sigma_i(E) dE$$

Dark matter in Molecular Clouds

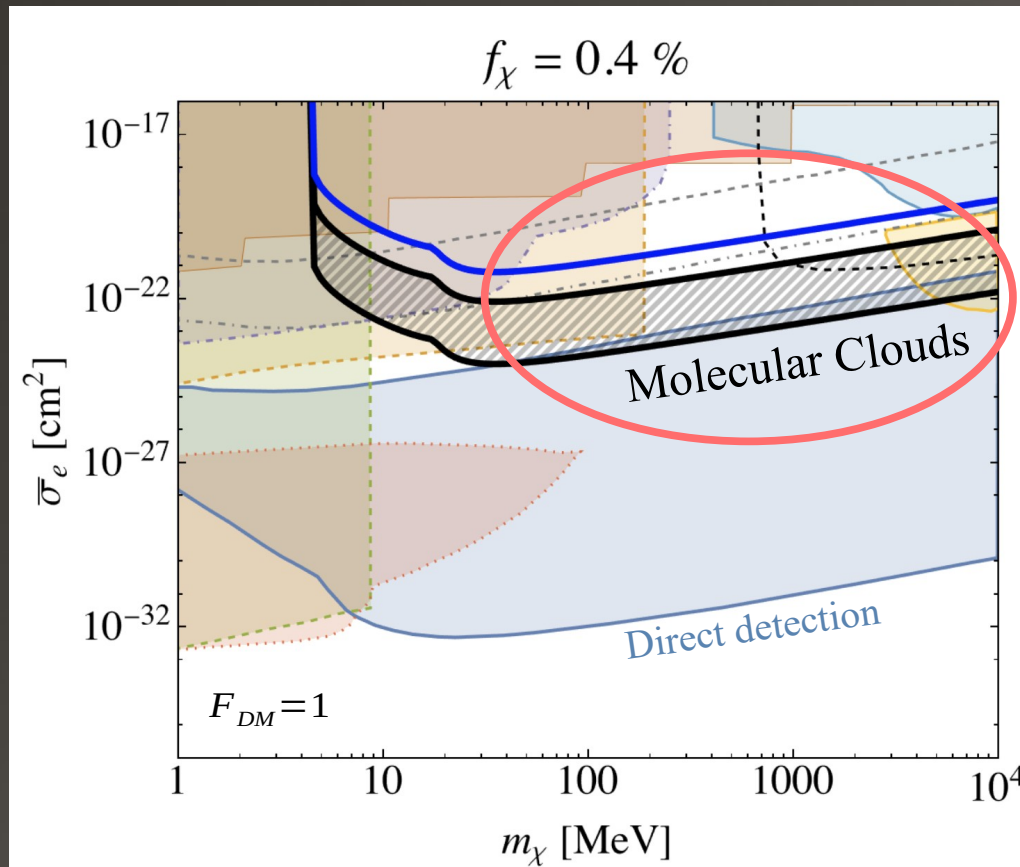


Constraints on DM w/ ultra-light mediator from dense (black) and diffuse (blue) molecular clouds. The hatched region represents the uncertainty in our bounds coming from the uncertainty in the inferred CR ionization rate due to gas depletion onto grain surfaces.

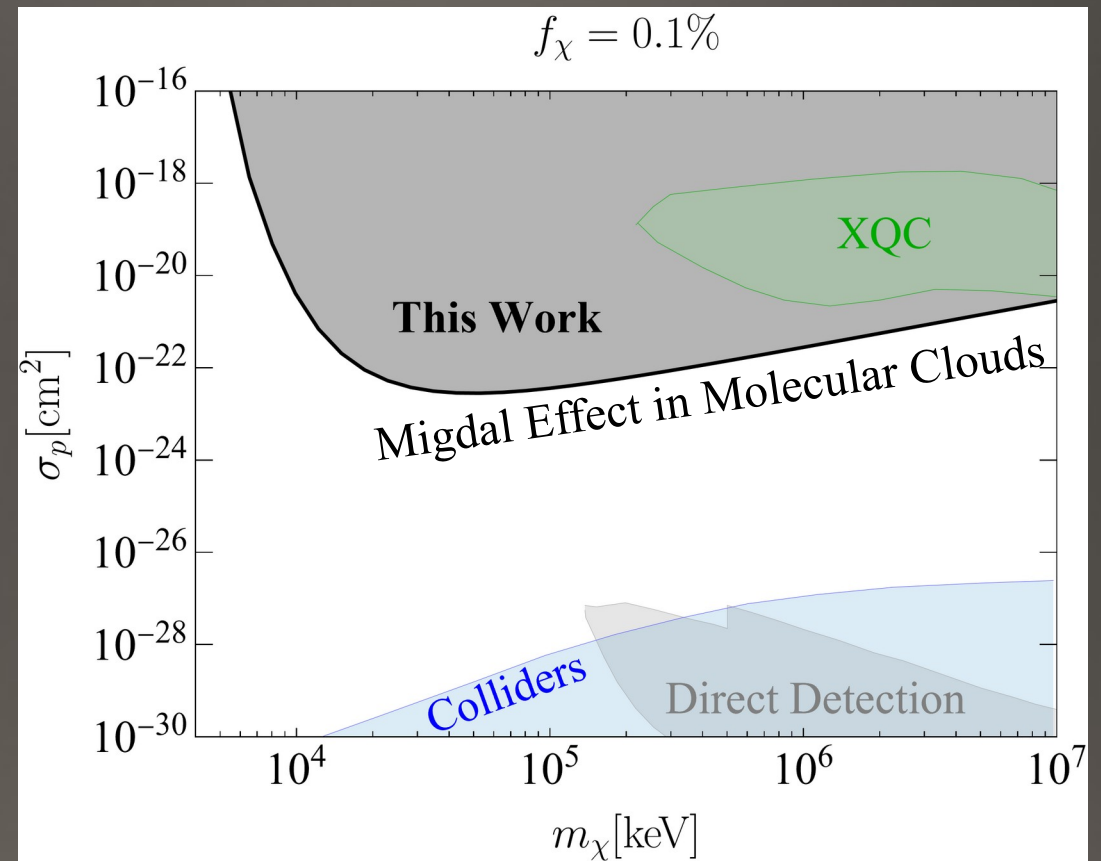
There would otherwise be an open window of parameter space where the dark matter is too strongly-coupled to be visible even by satellite experiments.

[Prabhu,CB: 2211.05787]

Dark matter in Molecular Clouds



[Prabhu, CB : 2211.05787]



[CB, Harris, Kahn, Prabhu: 2310.00740]

The Molecular Migdal effect(s) in *space*

Molecular cloud ionization (Thick lines) can constrain almost all remaining parameter space for a *strongly-coupled leptophilic* subcomponent of DM which would never make it to other detectors.

QDs – Cheap, tunable and scalable

QDot™ PbS Quantum Dots

\$399.00 - \$2,500.00

 Shipping worldwide

QDot™ PbS (Lead Sulfide) Quantum Dots, oleic acid capped, absorb the light from high energy photons up to near-infrared (NIR) range and re-emit in NIR range. The absorption/emission profiles can be tuned from 800 to 2200 nm, simply by changing nanoparticle sizes from 2 to 12 nm. This material has outstanding light absorption and photoelectrical properties, and is utilised for near-infrared (NIR) or short-wave infrared (SWIR) image sensors. For specific application convenience, two lines of QDs are available:

- With specific absorption peak in 800 - 2200 nm range
- With specific emission peak in 900 - 1600 nm range [Read more](#)

Absorption/Emission

Emission

Wavelength

1600 nm

Quantity

1g

Form


Toluene 10 mg/mL

[Reset](#)

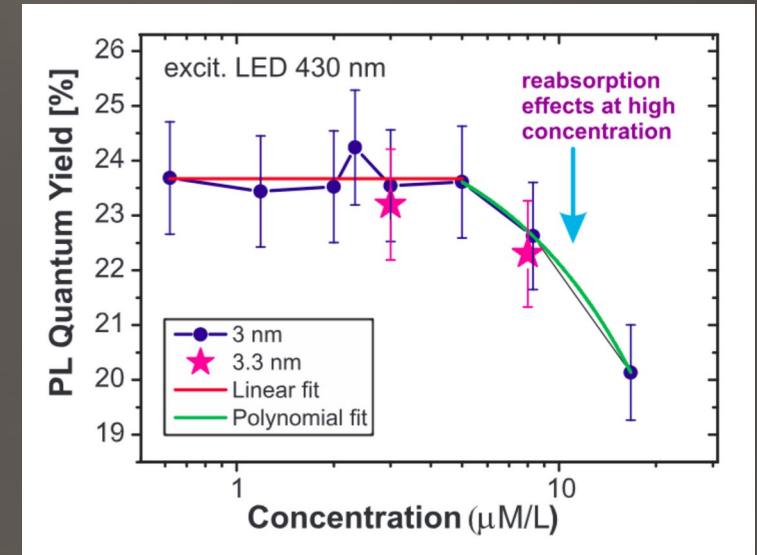
Price for chosen options

\$1,700.00

1

 Add to cart

[Contact with our expert](#)



Φ dependence on the solution concentration for 3nm and 3.3nm PbS QDs in toluene.

$$n_e \sim 10^{20} \text{ cm}^{-3} = 10^{23} \text{ L}^{-1}$$

Strongly Confining Quantum Dots

Semiconducting nano-spheres



$a \ll a_0$

$$E_{\text{confinement}} = \frac{\hbar^2 \pi^2}{2a^2} \left(\frac{1}{m_e} + \frac{1}{m_h} \right) = \frac{\hbar^2 \pi^2}{2\mu a^2}$$



$$E = E_{\text{bandgap}} + E_{\text{confinement}}$$

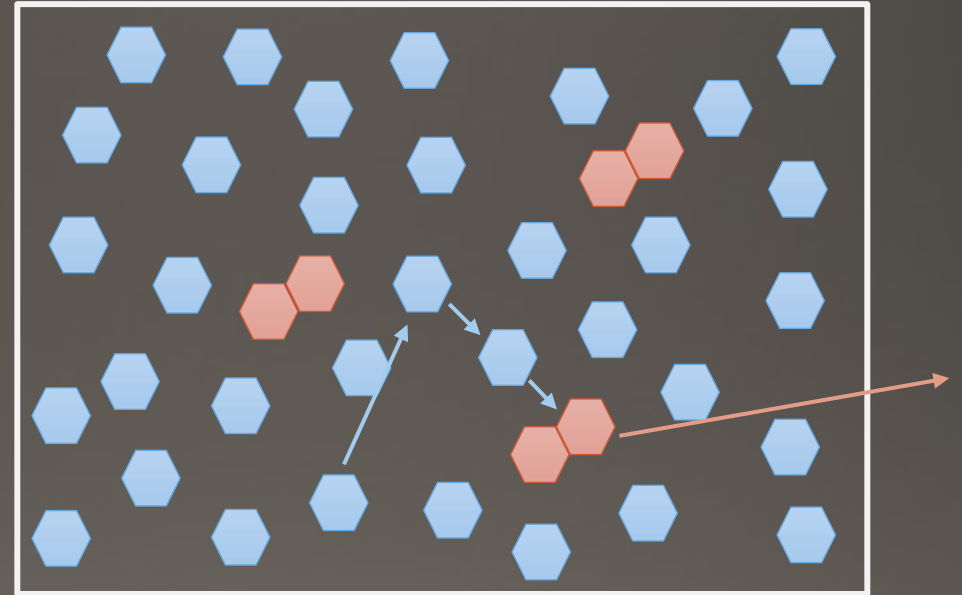
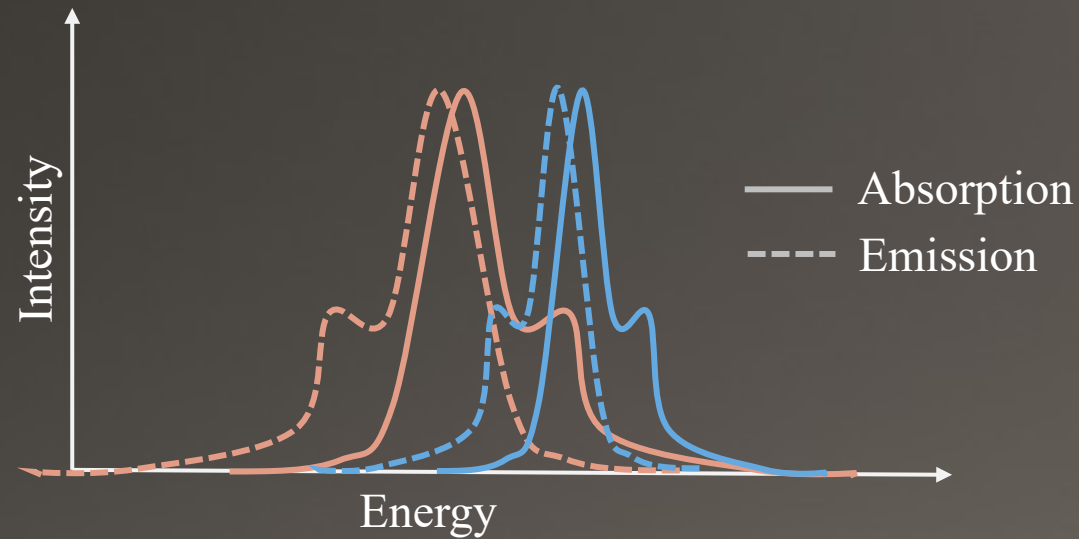
$$= E_{\text{bandgap}} + \frac{\hbar^2 \pi^2}{2\mu a^2}$$

$$E_{\text{kin}} \sim \frac{1}{r^2}$$

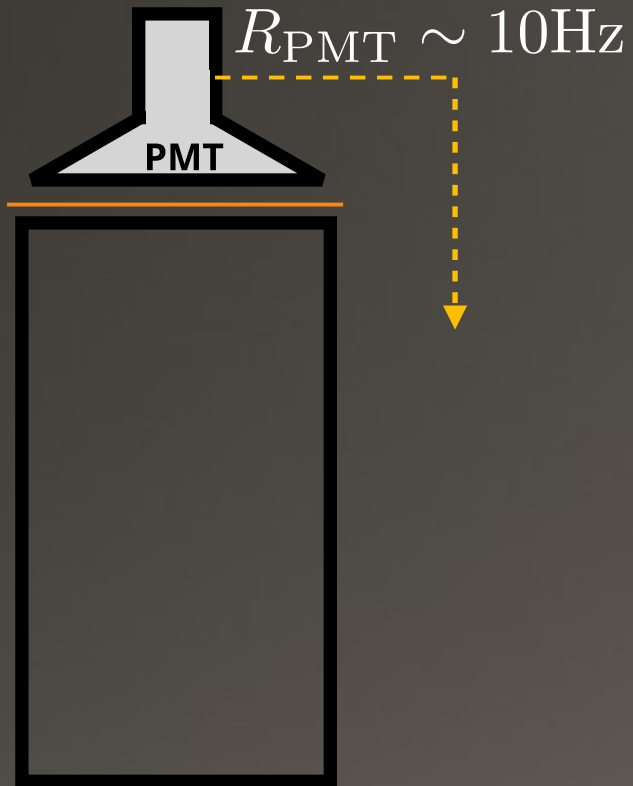
$$E_{\text{coulomb}} \sim \frac{1}{r}$$

Fluorescence: Binary Scintillators

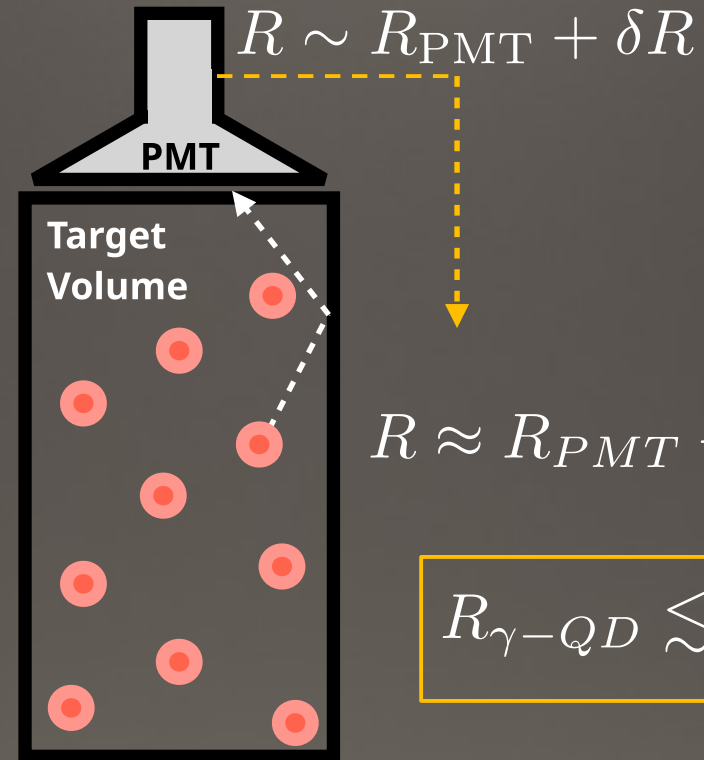
-  Solvent: Primary target starts the signal
-  Solute: Dilute fluor gets the signal out of the bulk



PbS QDs: Improvements



“Blind” mode



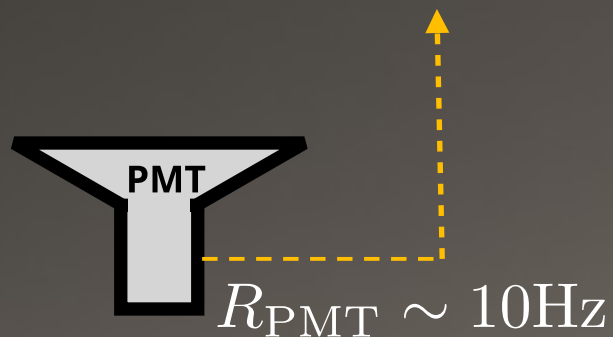
“Active” mode

$$R_{\gamma-QD} \lesssim \sqrt{R_{PMT}}$$

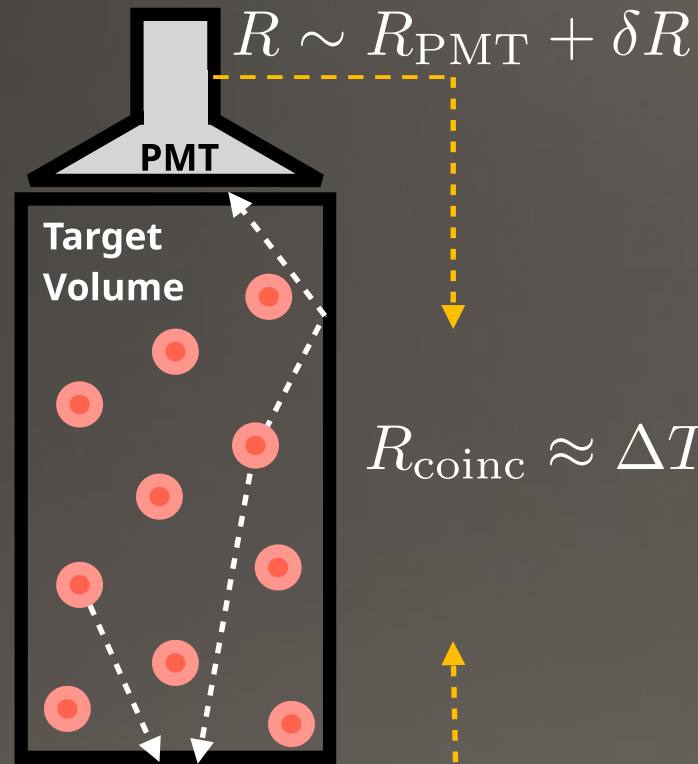
PbS QDs: Improvements



$$R_{\text{coinc}}^0 \approx \Delta T R_{PMT}^2$$



“Blind” mode

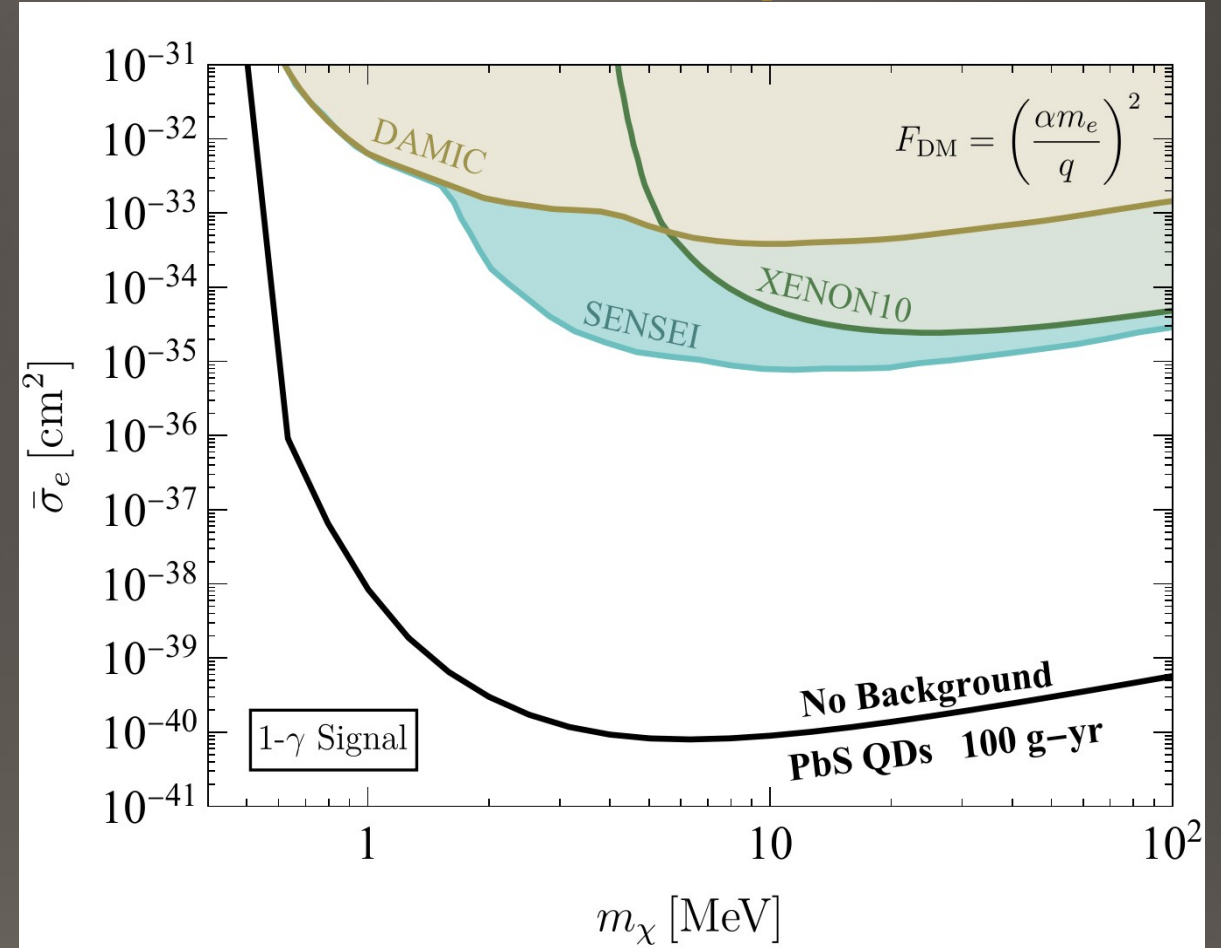
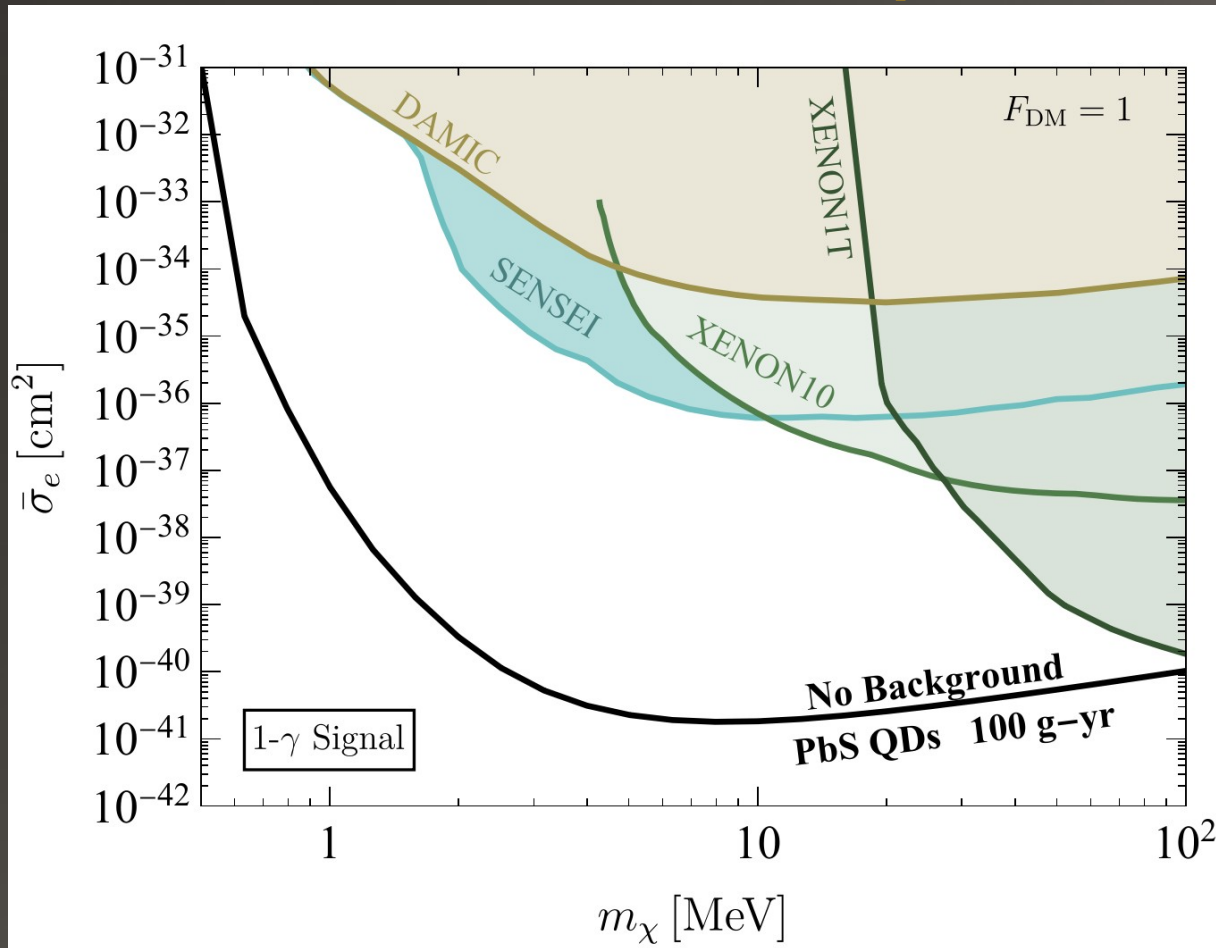


$$R_{\text{coinc}} \approx \Delta T R_{PMT}^2 + 2\Delta T R_{PMT} \delta R + R_{2\gamma-QD}$$

$$R_{2\gamma-QD} \lesssim \Delta T R_{PMT}^{3/2}$$

“Active” mode

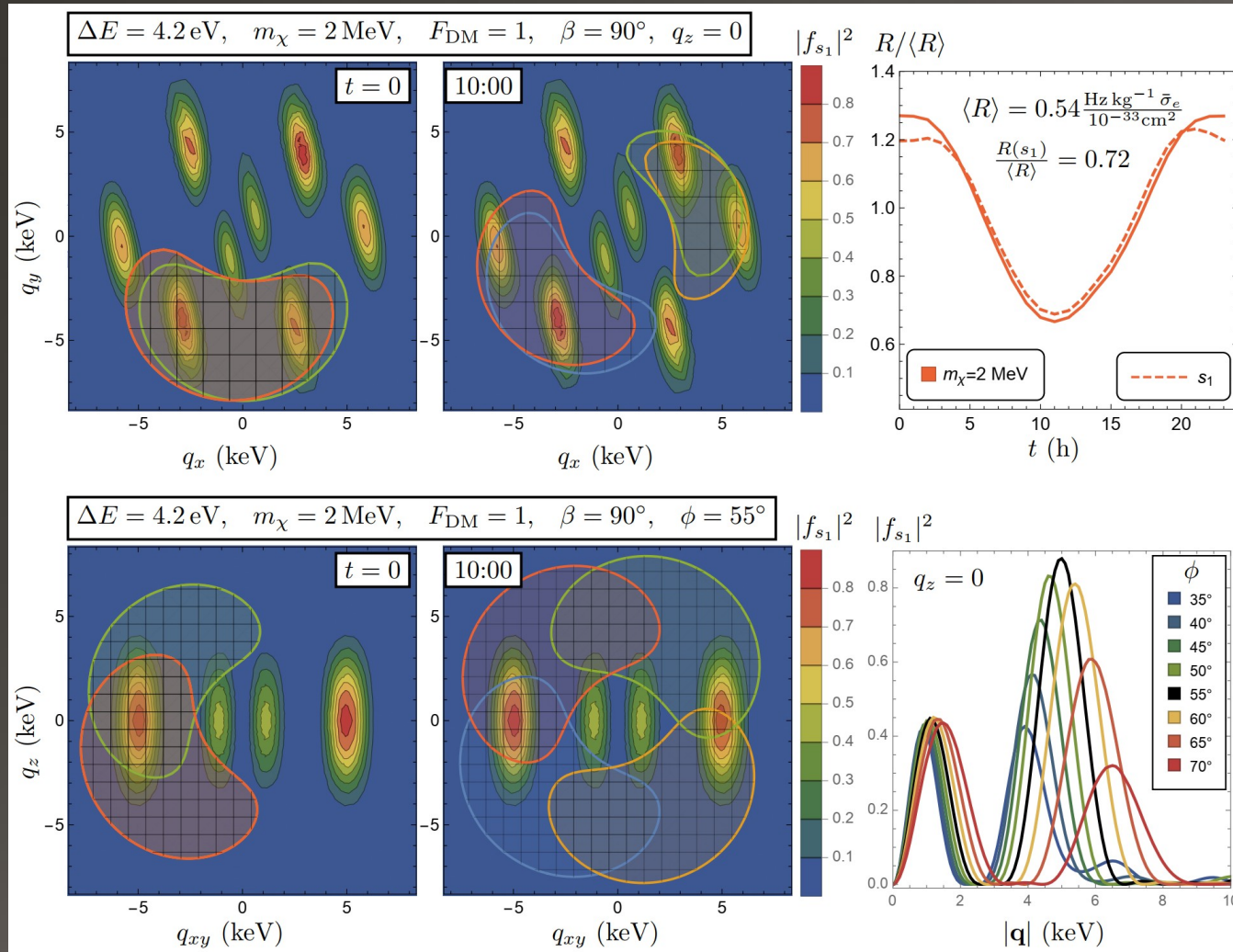
PbS QDs: Optimism for comparison



Blanco '22: 2208.05967

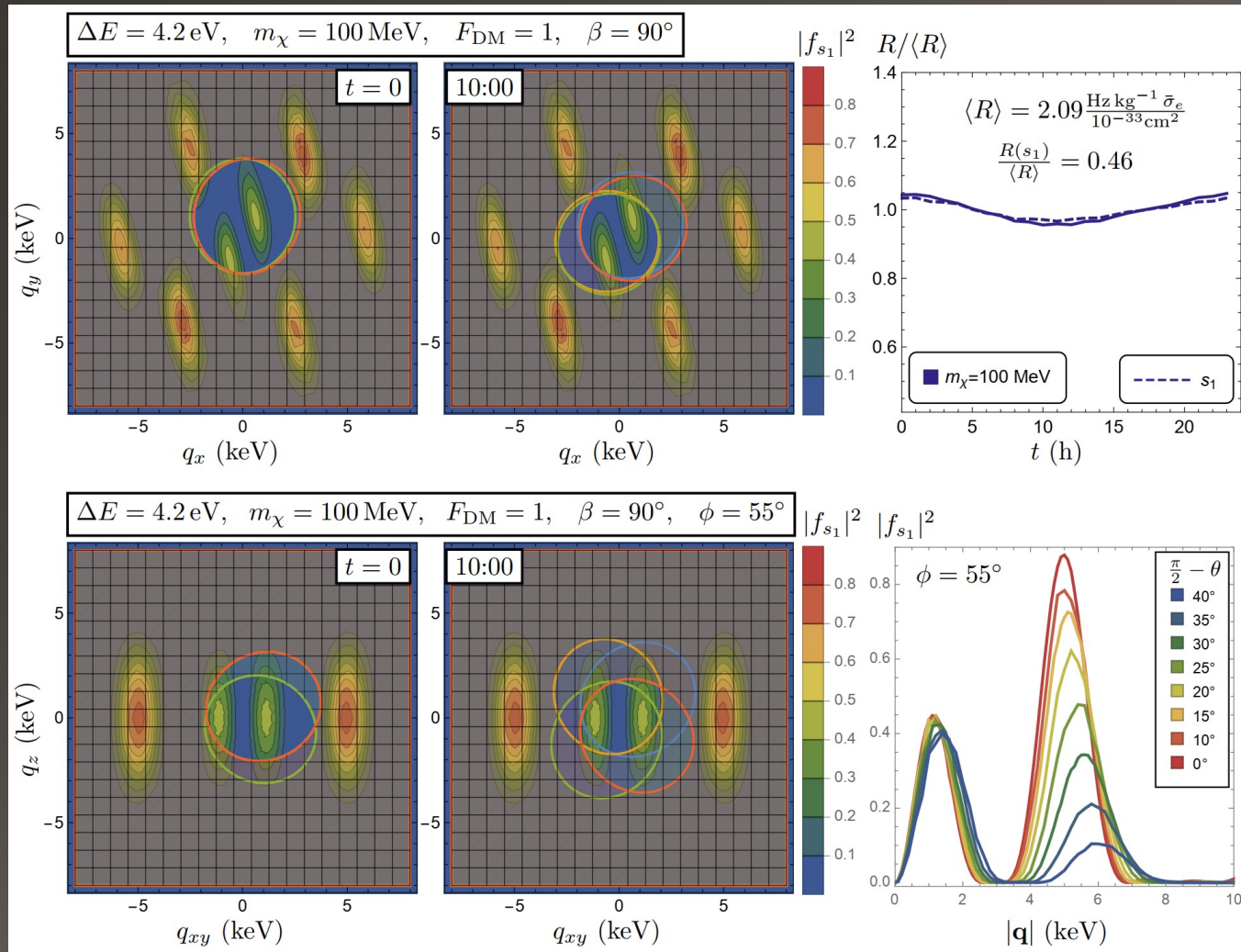
DM-Electron Scattering (no background 1-photon signal)

Daily Modulation: Small Mass



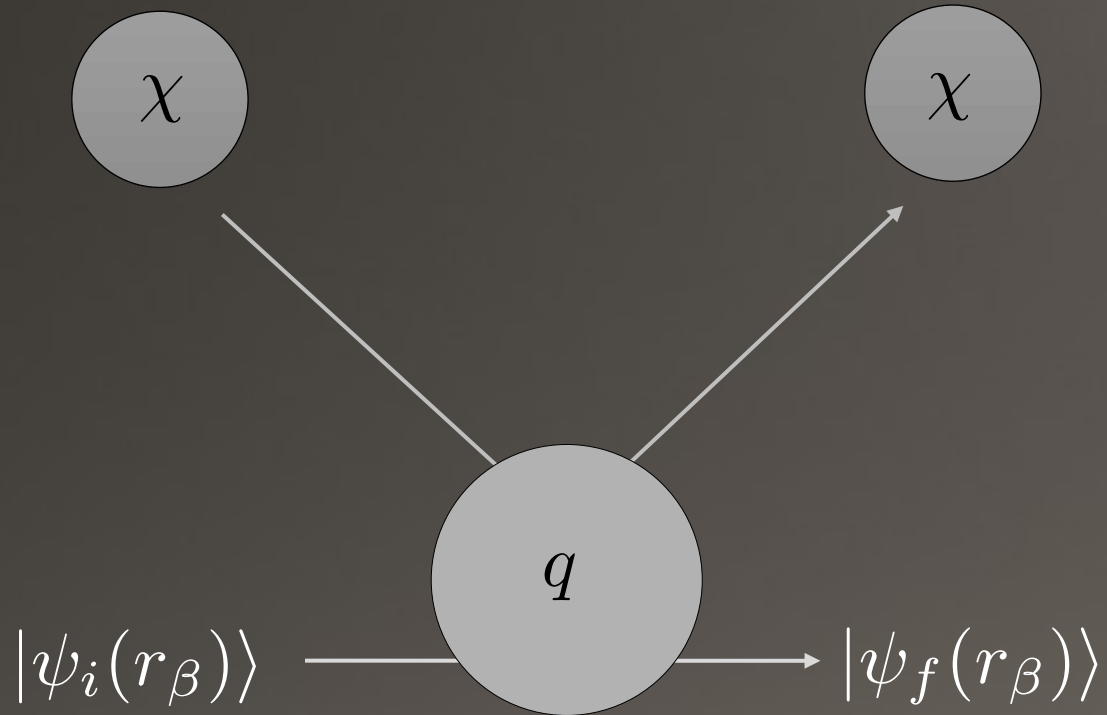
Molecular form factors and modulating rates for DM masses near threshold, $m_\chi = 2 \text{ MeV}$. In the contour plots, the gridded shaded regions indicate the kinematically accessible momentum transfers \vec{q} for the four molecules that comprise the unit cell of the crystal, shown at $t = 0$ and $t = 10 \text{ h}$. Here, \vec{q} is given in the molecular basis, $q_x = \vec{q} \cdot \hat{L}$, $q_y = \vec{q} \cdot \hat{M}$, and the kinematically accessible region is defined by $v_-(\vec{q}) < v_{\text{esc}}$.

Daily Modulation: Large Mass



Same as previous figure but for large DM masses, $m_\chi = 100 \text{ MeV}$. Only the nearly-spherical region near $q \sim 0$ with inner boundary $q_{\text{min}} \simeq 1.6 \text{ keV}$ is kinematically forbidden. As a result, the daily modulation amplitude is smaller, driven by the anisotropy of the inner secondary peaks and the tails of the primary peaks.

Electron Recoil: Charge Signal



Electron scattering

$$\Delta E_r = (m_\chi^2 / m_T) \times 10^{-6}$$

$$\Delta E \sim \mathcal{O}(\text{few eV}) \left(\frac{m_\chi}{1 \text{ MeV}} \right)^2$$

What has such transition energies?

- Semiconductor band gaps
- Maybe atomic ionization

Electrons in crystals (exciton generation)

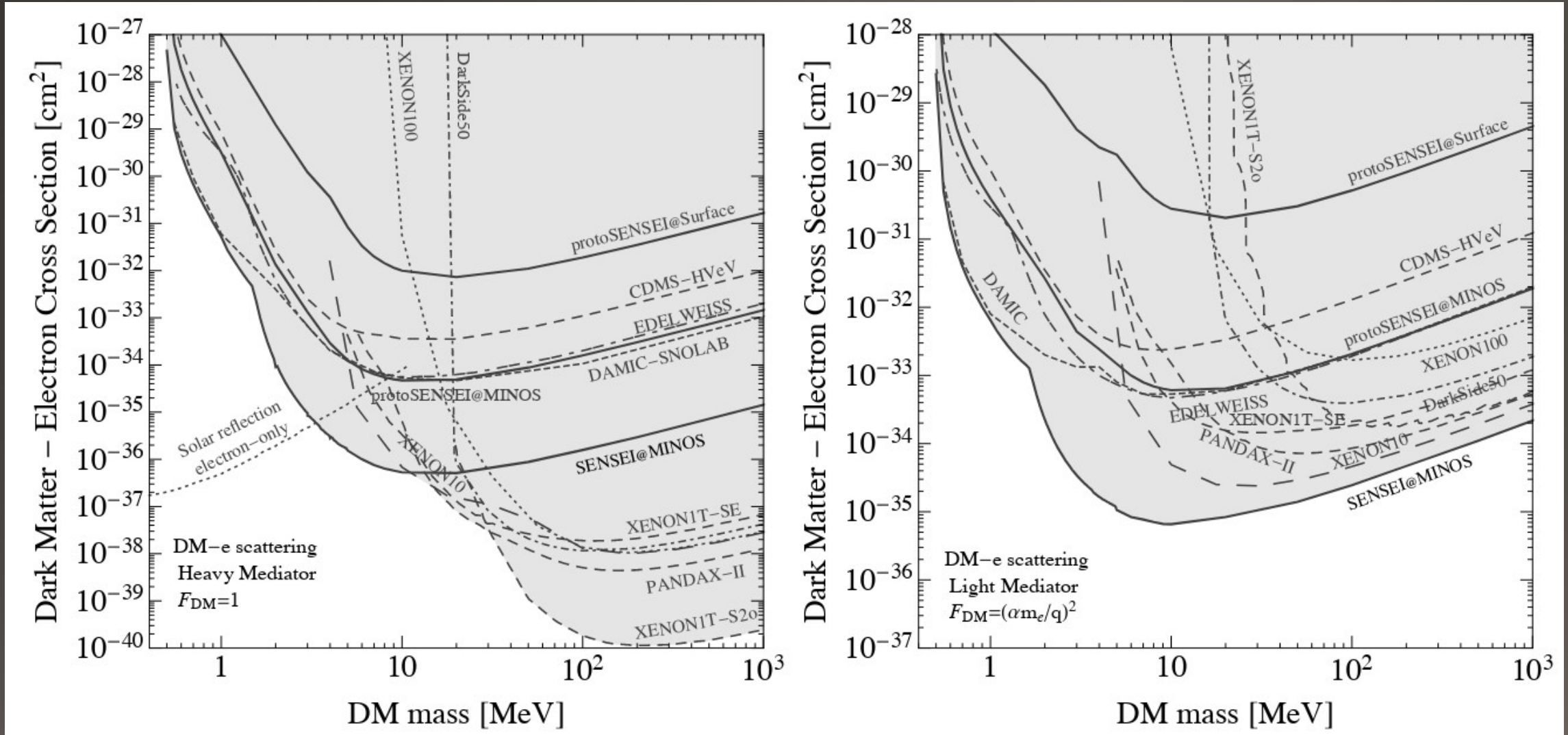
Electrons in atoms (ionization)

$$|\psi_i\rangle \sim u_v(r) e^{ik' \cdot r}$$

$$|\psi_f\rangle \sim u_c(r) e^{ik \cdot r}$$

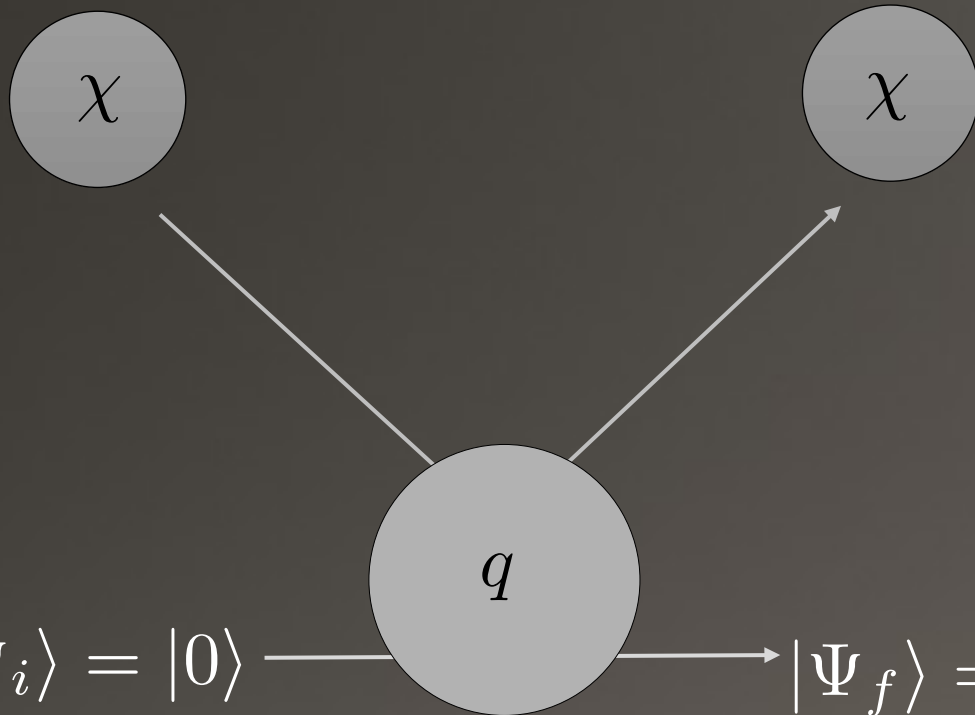
$$|\psi_i\rangle \sim \psi_{\text{STO}}(r_\beta) \quad |\psi_f\rangle \sim e^{ik \cdot r}, \quad r \gg a_0$$

Semiconductor CCDs



Essig R., et al. "Snowmass2021 Cosmic Frontier The landscape of low-threshold dark matter direct detection in the next decade" arXiv:2203.08297 (2022).

Nuclear Recoil: Phonon Signal



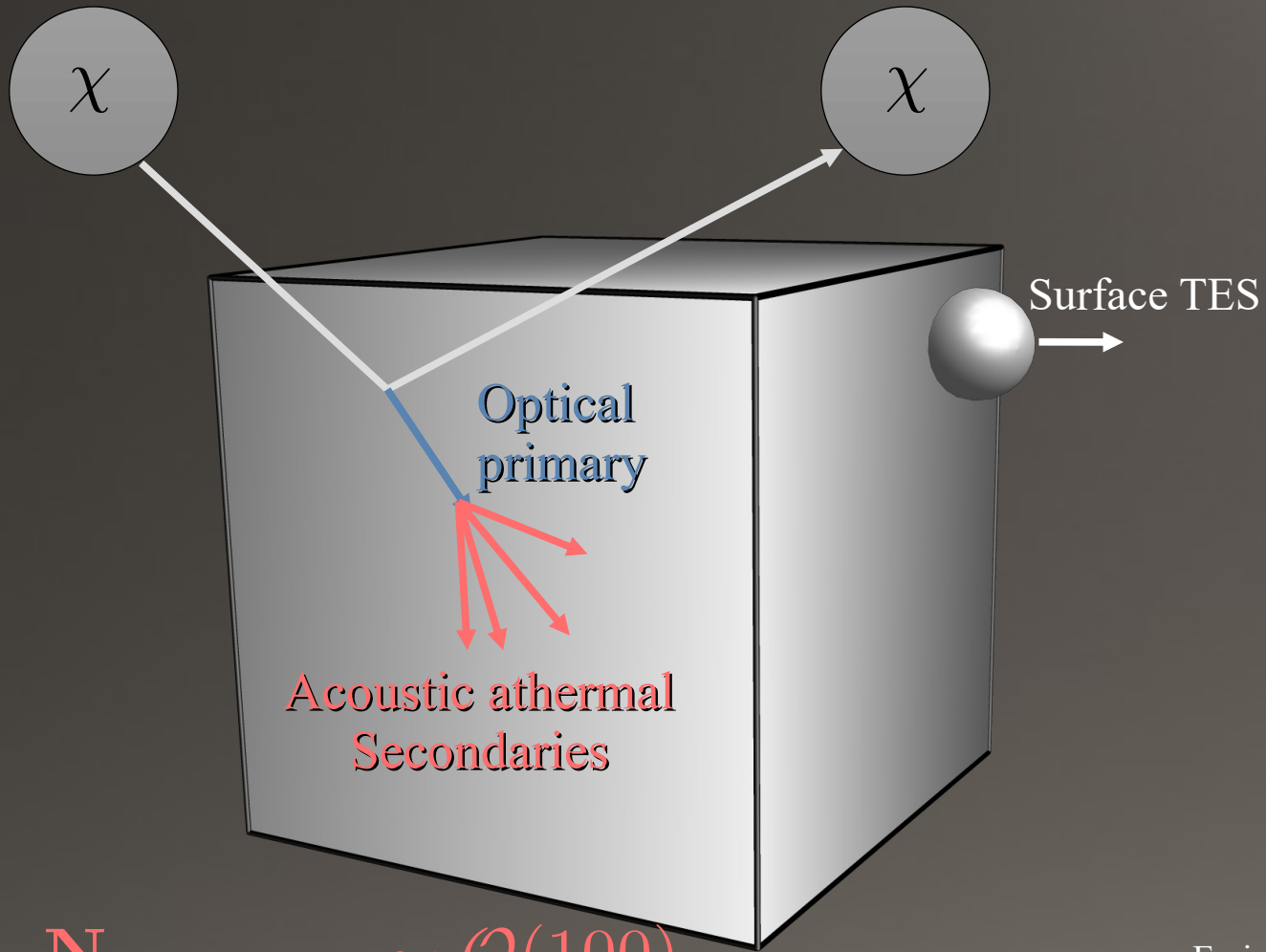
Nuclear scattering

$$\Delta E \sim \mathcal{O}(\text{few eV}) \left(\frac{m_\chi}{100 \text{ MeV}} \right)^2 \left(\frac{m_N}{130 \text{ GeV}} \right)^{-1}$$

$$\omega \sim \mathcal{O}(10\text{-}100 \text{ meV})$$

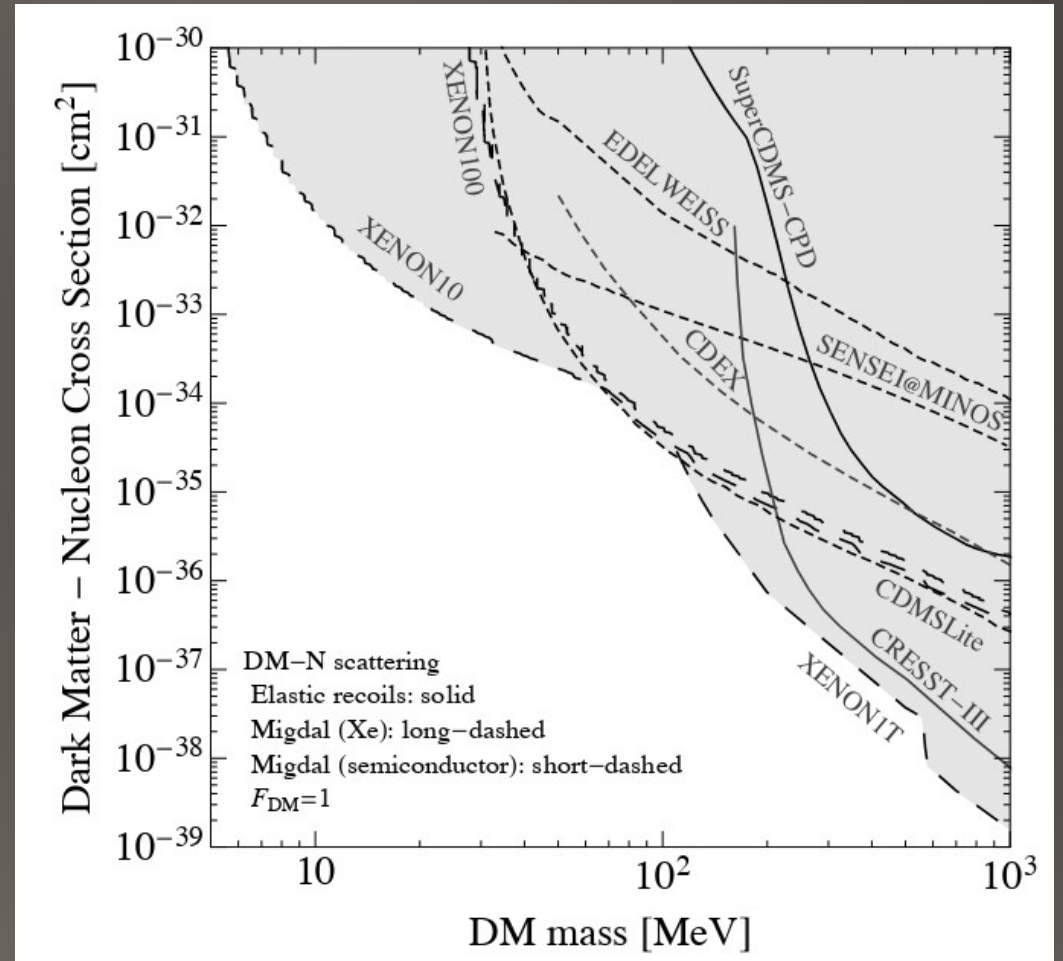
$$|\Psi_i\rangle = |0\rangle \longrightarrow |\Psi_f\rangle = a^\dagger(k) |0\rangle$$

Calorimeters



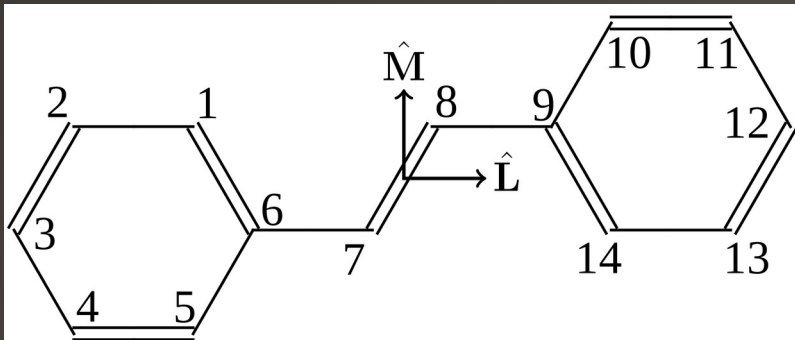
$$N_{\text{acoustic}} \sim \mathcal{O}(100)$$

$$E_0 \sim 10 - 100 \text{ meV}$$



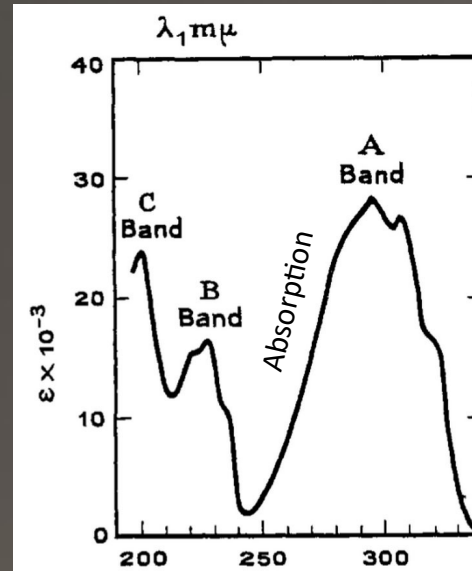
Essig R., et al. "Snowmass2021 Cosmic Frontier The landscape of low-threshold dark matter direct detection in the next decade" arXiv:2203.08297 (2022).

Directional Targets: Polyacenes



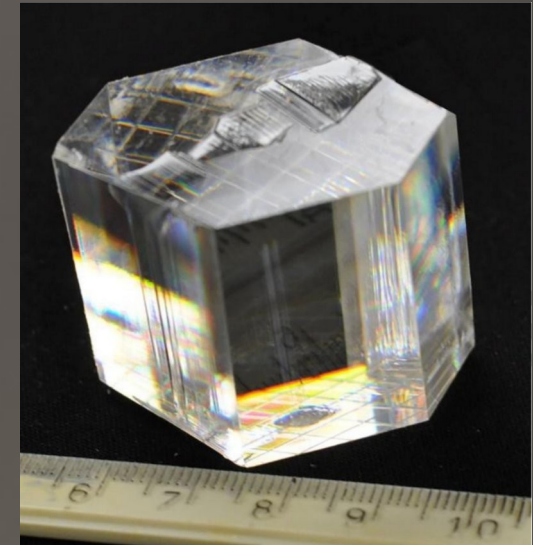
Trans-Stilbene

$$E_1 = 4.2\text{eV}$$



Beveridge & Jaffe '65

Dipole allowed E_1 !



Carman, et.al. '18 (J. of Crystal Growth)

Trans-Stilbene

s	Platt Symbol	Symmetry	ΔE [eV]	Configuration amplitudes			
s_1	1B	B_u	4.240	$d_{7,8} = 0.94,$	$d_{4,11} = -0.24$		
s_2	${}^1G^-$	B_u	4.788	$d_{7,10} = 0.53,$	$d_{5,8} = 0.53,$	$d_{6,11} = 0.37,$	$d_{4,9} = -0.37$
s_3	${}^1G^-$	A_g	4.800	$d_{7,9} = 0.53,$	$d_{6,8} = 0.53,$	$d_{5,11} = 0.37,$	$d_{4,10} = -0.37$
s_4	${}^1(C, H)^+$	A_g	5.137	$d_{7,11} = 0.41,$	$d_{5,9} = -0.41,$	$d_{6,10} = -0.41,$	$d_{4,8} = -0.59$
s_5	${}^1H^+$	B_u	5.791	$d_{5,10} = 0.54,$	$d_{6,9} = 0.54,$	$d_{7,12} = 0.33,$	$d_{3,8} = 0.33$
s_6	${}^1G^+$	A_g	6.264	$d_{7,9} = 0.68,$	$d_{6,8} = -0.68$		
s_7	${}^1C^-$	A_g	6.013	$d_{7,11} = 0.66,$	$d_{4,8} = 0.54,$		
s_8	${}^1G^+$	B_u	6.439	$d_{7,10} = 0.65,$	$d_{5,8} = -0.65$		

Table 1: The first eight excited states $s_{n=1\dots 8}$, with their energy eigenvalues $\Delta E(s_n)$ with respect to the ground state and coefficients $d_{ij}^{(n)}$ as calculated by Ting and McClure.

$$|s_n\rangle = \sum_{i,j>i} d_{ij}^{(n)} |\psi_i^j\rangle,$$

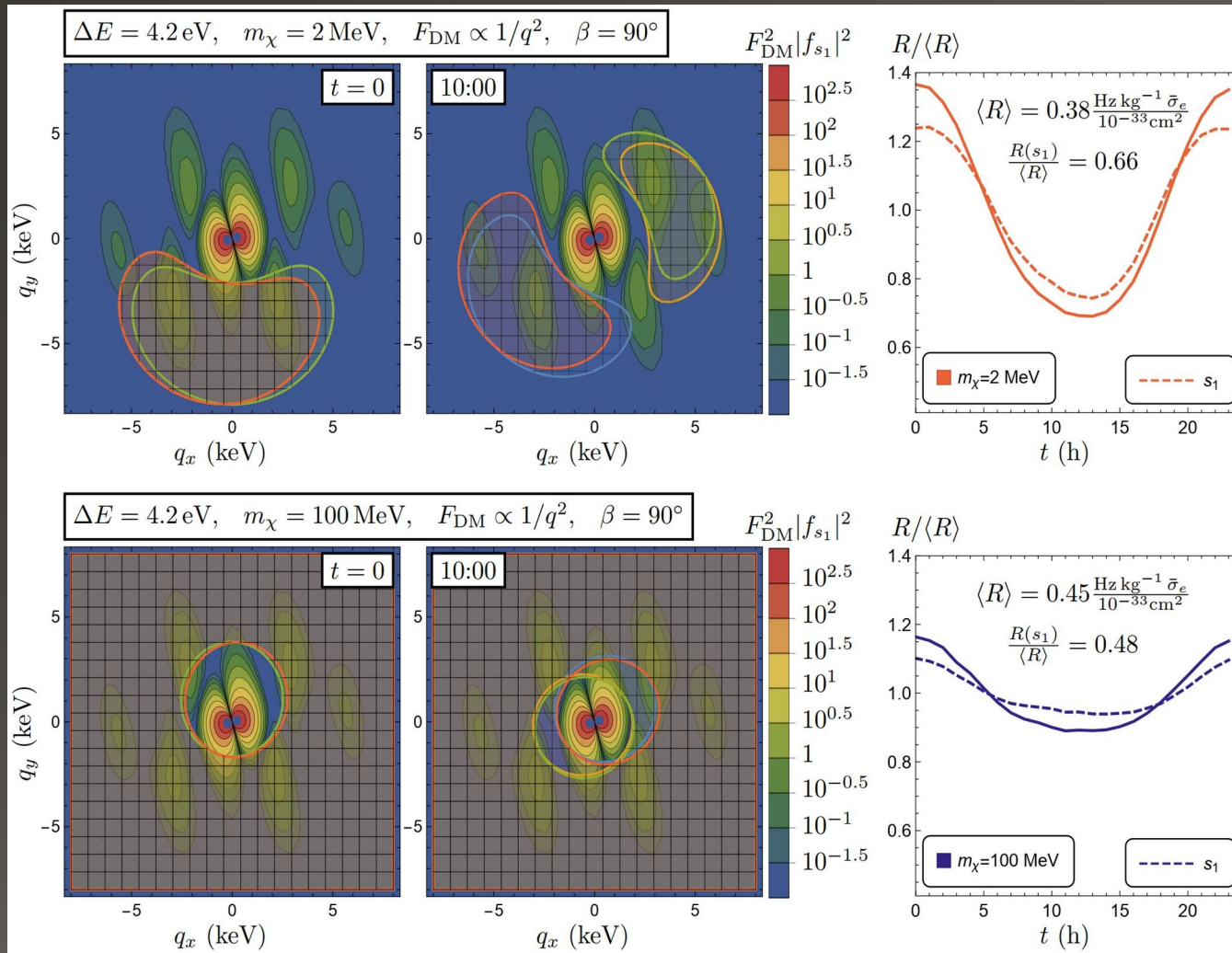
$$\sum_{ij} |d_{ij}^{(n)}|^2 = 1.$$

$$f_{g \rightarrow s_n}(\vec{q}) = \left\langle \psi_{s_n}(\vec{r}_1 \dots \vec{r}_{14}) \left| \sum_{m=1}^{14} e^{i\vec{q} \cdot \vec{r}_m} \right| \psi_G(\vec{r}_1 \dots \vec{r}_{14}) \right\rangle$$

$$= \sum_{ij} d_{ij}^{(n)} \langle \psi_i^j | e^{i\vec{q} \cdot \vec{r}} | \psi_G \rangle$$

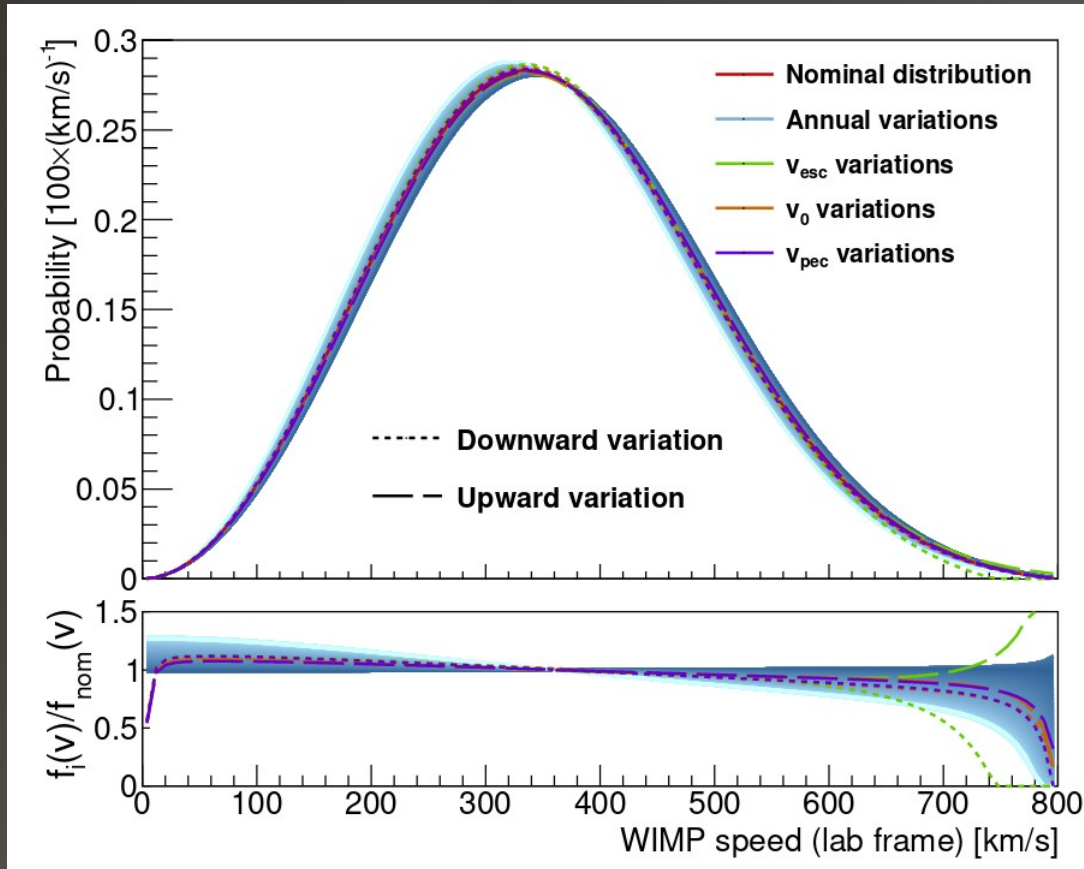
$$= \sqrt{2} \sum_{ij} d_{ij}^{(n)} \langle \Psi_j(\vec{r}) | e^{i\vec{q} \cdot \vec{r}} | \Psi_i(\vec{r}) \rangle.$$

Daily Modulation: Light Mediator

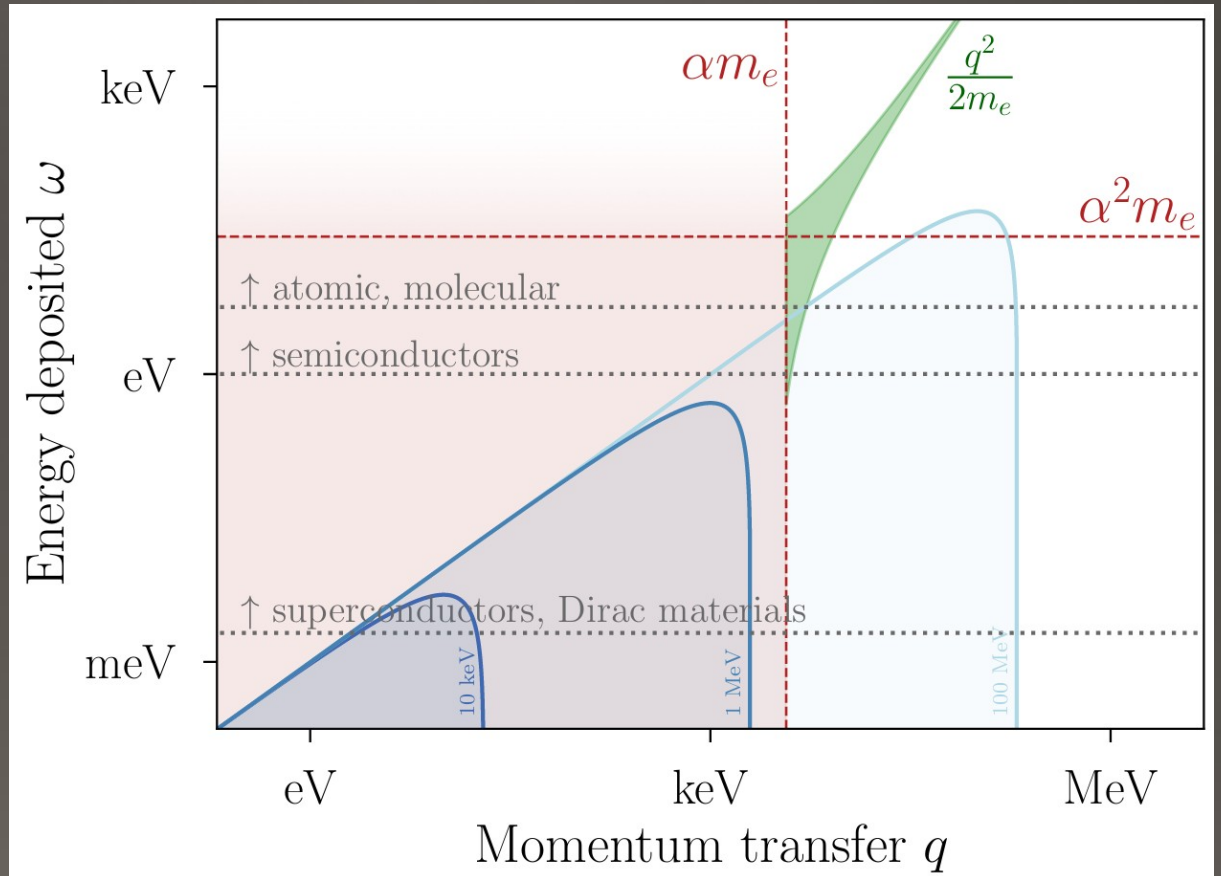


Same as previous figures (top) for a light mediator DM form factor $F_{\text{DM}} = (\alpha m_e/q)^2$. Here, the contour plots show $F_{\text{DM}}^2 |f(s_1)|^2$ which appears in the rate integrand; the scattering is dominated by the smallest kinematically-allowed q . **Top:** Molecular form factors with $q_z = 0$ and rate modulations for $m_\chi = 2 \text{ MeV}$. **Bottom:** Molecular form factors with $q_z = 0$ and rate modulations for $m_\chi = 100 \text{ MeV}$.

Local DM Phase Space



Baxter, D., et al. "Recommended conventions for reporting results from direct dark matter searches." *The European Physical Journal C* 81.10 (2021): 1-19.



Lin, Tongyan. "Sub-GeV dark matter models and direct detection." *SciPost Physics Lecture Notes* (2022): 043.